nature mental health

Article

https://doi.org/10.1038/s44220-024-00242-0

Defining the *r* factor for post-trauma resilience and its neural predictors

Received: 10 July 2023

Accepted: 25 March 2024

Published online: 22 April 2024

Check for updates

Sanne J. H. van Rooij[1] ✉, Justin L. Santos[1], Cecilia A. Hinojosa[1], Timothy D. Ely[1], Nathaniel G. Harnett[2,3], Vishnu P. Murty[4], Lauren A. M. Lebois[2,3], Tanja Jovanovic[5], Stacey L. House[6], Steven E. Bruce[7], Francesca L. Beaudoin[8,9], Xinming An[10], Thomas C. Neylan[11], Gari D. Clifford[12], Sarah D. Linnstaedt[10], Laura T. Germine[3,13,14], Kenneth A. Bollen[15], Scott L. Rauch[2,3], John P. Haran[16], Alan B. Storrow[17], Christopher Lewandowski[18], Paul I. Musey Jr.[19], Phyllis L. Hendry[20], Sophia Sheikh[20], Christopher W. Jones[21], Brittany E. Punches[22,23], Robert A. Swor[24], Jose L. Pascual[25,26], Mark J. Seamon[26,27], Erica Harris[28], Claire Pearson[29], David A. Peak[30], Roland C. Merchant[31], Robert M. Domeier[32], Niels K. Rathlev[33], Brian J. O'Neil[34], Leon D. Sanchez[31,35], Jutta Joormann[36], Diego A. Pizzagalli[2,3], John F. Sheridan[37,38], Steven E. Harte[39,40], Ronald C. Kessler[41], Karestan C. Koenen[42], Samuel A. McLean[10,43], Kerry J. Ressler[2,3] & Jennifer S. Stevens[1]

Although resilience is a dynamic process of recovery after trauma, in most studies it is conceptualized as the absence of specific psychopathology following trauma. Here, using the emergency department AURORA study (n = 1,835 with 63% women), we took a longitudinal, dynamic and transdiagnostic approach to define a static resilience (r) factor, which could explain greater than 50% of variance in mental well-being 6 months following trauma and a dynamic resilience factor, which represented recovery from initial symptoms. We then assessed its neurobiological profile across threat, inhibition and reward processes using functional magnetic resonance imaging collected 2 weeks post-trauma (n = 260). Our whole-brain and study-wide Bonferroni-corrected results suggest that resilience is promoted by activation of regions involved in higher-level cognitive functioning, reward valuation and salience detection in response to reward, whereas resilience is hampered by posterior default mode network activation to threat and reward. These findings serve to generate new hypotheses for brain mechanisms that could promote dynamic and multifaceted components of resilience following trauma.

In recent years, with high global levels of stress and trauma, the concept of resilience has accrued increasing interest, among scientists and the public alike, as a positive outlook after hardship or the ability to quickly recover from difficulties. Resilience is conceptualized in different ways and its scientific definition debated. It is defined in Webster as 'the capability of a strained body to recover its size and shape after deformation caused especially by compressive stress'[1] and is thought to require a set of complex and dynamic processes that allow individuals

A full list of affiliations appears at the end of the paper. ✉e-mail: sanne.van.rooij@emory.edu

to maintain psychological well-being in the face of adversity[2,3]. However, neurobiological research in the field of trauma, including our own work, has predominantly studied resilience as the absence of post-traumatic stress disorder (PTSD) or other trauma-related disorders in the aftermath of trauma or have used a trait-like resilience measure, such as the Connor–Davidson Resilience Scale[4–7]. While this prior work has been essential in understanding trauma resilience and its underlying neurobiological mechanisms, its unidimensional approach does not capture the complete picture of resilience, and it is unclear whether the identified mechanisms are related to protection from one specific disorder or more general well-being. Earlier conceptualizations of resilience, especially in the context of development, emphasize the dynamic aspect of the process and the importance of addressing its multiple components[8–10]. In this Article, we develop a novel methodology to account for both the dynamic and multifaceted components of resilience over the months following a traumatic event, identifying both transdiagnostic and specific features that can predict the recovery of mental health after this major life stressor.

A more complete understanding of the neurobiology of resilience across domains and its dynamics is needed for early interventions aiming to boost mental well-being in the aftermath of trauma. Human neuroimaging studies of resilience have consistently found lower threat reactivity in the amygdala and greater activation in prefrontal and hippocampal regions were associated with greater levels of resilience (reviewed in ref. 3). Furthermore, greater engagement of the salience network, including the dorsal anterior cingulate cortex (dACC) and insula early after trauma predicted better future mental health outcomes[3]. A common factor for resilience across multiple domains of adverse post-trauma sequaelae, however, has not been explored so far but could accelerate (neurobiological) research by providing important insights into protective mechanisms across such sequaelae and promote the development of potential early interventions for individuals at risk.

The idea of using one factor to explain variance across domains of psychopathology is not new. Following the *g* factor for general intelligence[11], the general factor of psychopathology, or *p* factor, was defined to explain cross-domain risks for psychopathology[12]. This transdiagnostic approach was developed to overcome challenges with identifying origins, biological markers or effective treatments for specific psychiatric disorders[13]. Furthermore, in healthy adolescents, principal component analyses (PCA) was used to predict adolescent resilient functioning across psychosocial domains[14]. The resilience factor (*r* factor) we sought to quantify is unique from the *p* factor in that it encompasses the early aftermath of trauma and seeks to understand heterogeneity among a broader population in early responses to a major environmental stressor. Further, instead of constant factor over time, the *r* factor includes two components to account for the change following trauma (Fig. 1): (1) the static *r* factor, representing mental well-being 6 months post-trauma and corresponding to definitions of absence of unidimensional symptoms in prior studies; and (2) the dynamic *r* factor, representing recovery from initial symptoms early post-trauma period (2 weeks) relative to 6 months post-trauma. The dynamic *r* factor is created to account for the dynamic nature of resilience between 2 weeks and 6 months post-trauma, the time when resilient and high-risk groups diverge[15].

We not only expected that key transdiagnostic mechanisms would facilitate resilience in the aftermath of a traumatic event, but we further hypothesized that resilience may be multifaceted, such that some symptoms may follow a different pattern of recovery than those that are linked to a central transdiagnostic indicator of recovery distress. This stands in contrast with the field of resilience research so far, which has focused on a single construct of 'stress resilience', although this has been operationalized in different ways across investigator groups and species. In addition to the main *r* factor, we investigated secondary components that diverge in their occurrence and recovery pattern from the *r* factor and explain substantial variance in the aftermath of trauma, potentially representing different types of resilience. After isolating these shared features of resilience, we aimed to identify brain-based predictors of these more circumscribed components of resilience and assessed the functional neurobiological profile across inhibition, threat and reward-related processes.

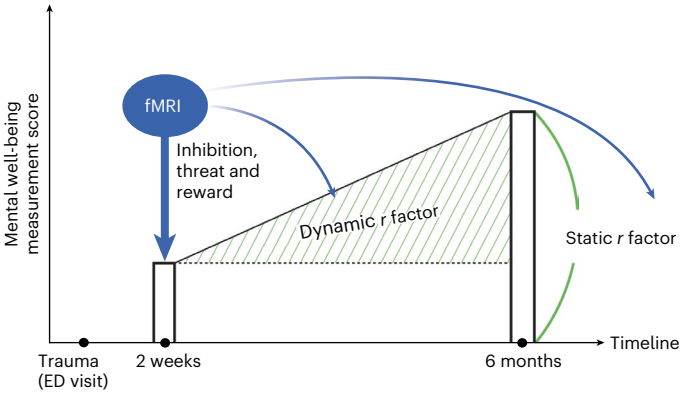

Fig. 1 | Schematic overview of the study and the dynamic and static *r* factor. A schematic overview of the study and a graphic explanation of the static and dynamic *r* factor scores. Mental well-being is measured with 45 items on six clinical domains, that is, anxiety, depression, PTSD, impulsivity, sleep and alcohol and nicotine use.

Results

The data for the current analyses were collected as part of the multisite emergency department (ED) AURORA study[16]. Civilians with recent trauma exposure brought to one of 29 participating EDs across the United States were recruited for this large, longitudinal study (details in refs. 16,17). Participants with complete 6-month item-level clinical data were included in the current analyses (n = 1,835 with 1,175 women; Table 1). Both a priori and post hoc power analyses were computed (Supplementary Methods and Supplementary Tables 1 and 2).

PCA defining resilience

The *r* factor was defined on the basis of item-level data of mental well-being across domains of anxiety, depression, PTSD, sleep, impulsiveness, alcohol and nicotine use collected 2 weeks and 6 months following trauma. Using PCA of self-reports from 6 months post-trauma, three components were extracted based on an inflection point of the scree plot, along with a secondary threshold of eigenvalues >2 (Table 2). The main *r* factor for global stress reflected general mental well-being following trauma (eigenvalue of 23.52). Two additional components were identified, one labeled as reminder acceptance (eigenvalue of 2.39), which represents low levels of reexperiencing and avoidance of reminders of the traumatic event, and a second labeled behavioral control (eigenvalue of 2.17), which represents low levels of the impulsivity, risk taking, loss of control and feeling rejected, that often follow a major stressor. Notably, the highest loadings for each of the three components bridged multiple instruments and domains, suggesting that the data support a transdiagnostic approach, though the secondary components pivot more to specific domains. Males had greater mean scores of reminder acceptance (t = 6.03, P < 0.001), whereas females had greater behavioral control scores (t = −3.92, P < 0.001). Older age correlated with greater scores on *r* (r = 0.08, P < 0.001) and behavioral control (r = 0.13, P < 0.001) but lower reminder acceptance (r = −0.13, P < 0.001). Because age and sex contributed to variance of interest and indeed showed associations with the scores, they were not again included as covariates in the neuroimaging analyses, though sensitivity analyses were conducted to test the influence of age and sex as well as trauma-related variables. Childhood trauma correlated negatively with

all components; however, correlation values for reminder acceptance were small and not statistically significant for childhood neglect. The trait resilience positively correlated with *r* and behavioral control but not with reminder acceptance (details in Supplementary Results and Supplementary Table 3).

Dynamic resilience was calculated by estimating scores for the 2-week data on the basis of the loadings derived from the 6-month data and computing difference scores. There was a statistically significant increase in the score over time (2 weeks to 6 months) for the *r* factor ($t = -3.7$, $P < 0.001$) and reminder acceptance ($t = -21.0$, $P < 0.001$) but a decrease for behavioral control ($t = 8.6$, $P < 0.001$; see Supplementary Table 4 for details). The static and dynamic resilience scores were all statistically significantly correlated (all $P < 0.001$ but shared only 19% to 27% of variance; Supplementary Results 4).

Functional neuroimaging

We then assessed the functional neurobiological profile of the components across inhibition, threat and reward-related processes using functional magnetic resonance imaging (fMRI) scans that were collected at 2 weeks post-trauma for a subset of individuals ($n = 445$ included in analyses and $n = 260$ after excluding for anatomical concerns, lack of behavioral responses or available data, excessive motion, technical issues or incomplete *r* factor data). The static and dynamic resilience scores did not significantly differ between the overall and neuroimaging dataset (Supplementary Table 5).

We investigated the potential confounding influence of trauma severity (injury severity score (ISS) and pain in the ED), and trauma type on the neuroimaging resilience score analyses. We observed no association between trauma severity and the static or dynamic *r* factor score, reminder resilience or behavioral control (Supplementary Results and Supplementary Table 6). Pain in the ED significantly correlated with static trauma reminder resilience scores ($r = -0.33$, $P < 0.001$) but not with other static or dynamic resilience scores. There was also no association between trauma type and the resilience scores.

Neuroimaging data were collected at five sites with comparable parameters (see Supplementary Table 7 for details). Functional images were preprocessed with fMRIPrep, version 1.2.2 (ref. 18). First-level statistical modeling was conducted in SPM12. Regions of interest (ROIs) were selected in the larger AURORA study[17] and consistently used here. ROIs included the hippocampus and ventromedial prefrontal cortex (vmPFC) for inhibition, the amygdala, hippocampus, sugbenual and dACC for threat and nucleus accumbens, amygdala, orbitofrontal cortex (OFC) for reward (see Methods for details). The mean across all voxels in each ROI was extracted from first-level contrasts using REX[19]. Whole-brain group-level maps were created for inhibition, threat and reward contrasts and included dummy variables for site. A factorial design with multiple regressors was used to examine the voxel-level correlations between the contrast estimates for inhibition, threat and reward with each of the continuous resilience scores as dimensional regressors in separate models.

***r* factor.** ROI analyses showed that greater OFC reactivity to monetary reward 2 weeks post-trauma predicted greater static and dynamic* *r* factor scores (Fig. 2a and Supplementary Materials 8). As indicated by the asterisk, the dynamic *r* factor correlation survives additional correction for multiple comparisons across all nine ROIs, three components and for the two types of resilience (54 tests, $P < 0.0009$). There were no statistically significant associations for regions selected for the threat or inhibition tasks.

The whole-brain analyses (Fig. 2b, Table 3 and Supplementary Materials 8) showed that during reward processing, the static *r* factor positively correlated with activation in the right superior temporal gyrus (STG) and insula, such that greater reward-related activation in these regions 2 weeks post-trauma was related to greater levels of resilience 6 months post-trauma. Additionally, the static *r* factor score negatively correlated with activation in the bilateral precuneus* and left inferior parietal lobe (IPL)* reactivity, such that less reward-related activation was related to greater resilience. As indicated by an asterisk, the negative correlations were robust to additional study-wide Bonferroni corrections for all whole-brain analyses, across three tasks, three components and static and dynamic resilience (18 tests, $P < 0.0028$). No significant correlations with the inhibiton or threat tasks was observed.

Table 1 | Demographic data

	Total sample	Imaging sample
	n=1,835	*n=260*
	Mean (s.d.) or *N* (%)	Mean (s.d.) or *N* (%)
Age	37.4 (13.6)	35.4 (13.0)
Sex at birth		
Male	660 (36%)	93 (36%)
Female	1175 (64%)	167 (64%)
Race		
Hispanic white	185 (10%)	34 (13%)
Non-Hispanic white	662 (36%)	93 (36%)
Non-Hispanic Black	916 (50%)	118 (45%)
Non-Hispanic other	65 (4%)	13 (5%)
Marital history		
Current or previous marriage	760 (42%)	85 (33%)
Never married	1,063 (58%)	174 (67%)
Missing	12 (1%)	1 (0.4%)
Education		
High school or less	209 (11%)	19 (7%)
Some college or more	1,620 (88%)	241 (93%)
Missing	6 (0.3%)	0
Currently employed		
No	476 (26%)	73 (28%)
Yes	1,255 (68%)	173 (67%)
Missing	104 (6%)	41 (5%)
Income		
≤$35,000 yearly	1,089 (59%)	143 (55%)
>$35,000 yearly	635 (35%)	101 (39%)
Missing	111 (6%)	16 (6%)
Trauma severity[#]	2.5 (2.0)	2.4 (2.0)
Pain in the ED[&]	6.5 (4.6)	6.2 (4.4)
Trauma type[%]		
Motor vehicle accident	1,349 (73.5%)	182 (70.0%)
Physical assault	164 (8.9%)	27 (10.4%)
Sexual assault	9 (0.5%)	1 (0.4%)
Fall ≥10 ft	32 (1.7%)	6 (2.3%)
Other (ten categories including poisoning, burns and animal related)	281 (15.3%)	44 (16.9%)
Childhood trauma (CTQ-SF)	9.5 (8.9)	9.2 (9.7)

[#]Trauma severity is measured with the ISS and the AIS. The ISS takes into account multiple injuries and regions. The AIS is an international standard tool for ranking the severity of injuruy on a 6-point ordinal scale. The score equals the sum of the squares of the highest AIS scores. [&]Pain in the ED is measured with the Numeric Pain Rating Scale, and the question 'the number of body parts with pain (0–18)' is used as continuous variable. [%]Trauma type was quantified by assigning each individual's trauma to one of the 22 specific categories. The categories were numbered and used as a categorical variable in the sensitivity analyses. The traumas are summarized in five broad trauma type categories for clarity of display.

https://doi.org/10.1038/s44220-024-00242-0

Table 2 | Varimax rotation component loadings for the *r* factor, reminder acceptance and behavioral control factors (*n*=1,835)

Clinical domain	Item	Varimax rotation component loading		
		r factor	Reminder acceptance	Behavioral control
	Percent variance explained by factor	52.3%	5.3%	4.8%
Anxiety	Anxious	**−0.63#**	**−0.38**	−0.11
Anxiety	Tense	**−0.63#**	**−0.39**	−0.08
Anxiety	Trouble to relax	**−0.63#**	**−0.37**	−0.08
Anxiety	Worry about things	**−0.64#**	**−0.36**	−0.04
Depression	Depressed	**−0.79***	−0.29	−0.16
Depression	Failure	**−0.81****	−0.26	−0.25
Depression	Helpless	**−0.80****	−0.29	−0.25
Depression	Hopeless	**−0.81****	−0.26	−0.26
Depression	Nothing interest	**−0.70***	**−0.36**	−0.25
Depression	Nothing to look forward	**−0.81****	−0.23	−0.26
Depression	Sad	**−0.77***	**−0.31**	−0.13
Depression	Unhappy	**−0.79***	−0.28	−0.16
Depression	Worthless	**−0.81****	−0.27	−0.29
Impulsivity	Act without thinking when excited	−0.24	−0.22	**−0.78***
Impulsivity	Act without thinking when upset	**−0.33**	−0.24	**−0.66#**
Impulsivity	Feeling rejected	**−0.33**	−0.23	**−0.68#**
Impulsivity	Lose control	−0.29	−0.24	**−0.77***
Impulsivity	See things through	−0.01	−0.06	−0.01
Impulsivity	Think carefully	−0.07	−0.14	−0.10
Impulsivity	Think things over	−0.18	−0.16	−0.22
Impulsivity	Unfinished tasks	**−0.38**	−0.22	−0.29
PTSD	Avoid reminders	**−0.30**	**−0.78***	−0.16
PTSD	Avoid stress experience	**−0.31**	**−0.79***	−0.16
PTSD	Bad dreams	**−0.34**	**−0.73***	−0.17
PTSD	Blaming self	**−0.51**	**−0.60#**	−0.20
PTSD	Difficulty concentrate	**−0.52**	**−0.43**	−0.24
PTSD	Disturbing memories	−0.34	**−0.77***	−0.12
PTSD	Feeling cut off	**−0.68#**	**−0.42**	−0.19
PTSD	Feeling fear	**−0.58**	**−0.58**	−0.19
PTSD	Feeling irritable	**−0.56**	**−0.47**	−0.28
PTSD	Feeling jumpy	**−0.31**	**−0.58**	−0.26
PTSD	Feeling Upset	**−0.35**	**−0.79***	−0.10
PTSD	Lack positive emotions	**−0.69#**	**−0.44**	−0.27
PTSD	Loss of interest	**−0.65#**	**−0.47**	−0.20
PTSD	No one can be trusted	**−0.63#**	**−0.51**	−0.24
PTSD	Reliving event	−0.27	**−0.77***	−0.23
PTSD	Sleep problems	**−0.39**	**−0.40**	−0.11
PTSD	Strong physical reactions	**−0.33**	**−0.78***	−0.17
PTSD	Super alert	−0.22	**−0.58**	−0.17
PTSD	Taking risks	**−0.30**	**−0.30**	**−0.58**
PTSD	Trouble remembering	**−0.34**	**−0.58**	−0.27
Sleep	Difficulty staying awake in the day	−0.21	−0.20	−0.15
Sleep	Sleep Prob Diff Get Things Done	−0.29	−0.24	−0.29
Substance	Number days nicotine	−0.07	−0.10	−0.07
Substance	Number days alcohol	−0.08	0.01	−0.13

The strength of the component loading is indicated by two asterisks (**) for <−0.8, one asterisk for <−0.7, one number sign for <−0.6, and bold for any item with component loading <−0.3.

The dynamic *r* factor showed correlations with the reward and threat tasks, but no correlations were observed with the inhibition task (Fig. 2b, Table 3 and Supplementary Materials 8). During reward processing, the dynamic *r* factor positively correlated with activation in the bilateral superior frontal gyrus (SFG)*, bilateral insula*, left superior medial gyrus (SMG)* and dACC*, such that greater reward-related activation 2 weeks post-trauma predicted a greater increase in the *r* factor between 2 weeks and 6 months post-trauma. During threat processing, the *r* factor was negatively correlated with activation in the bilateral IPL*, such that lower threat reactivity 2 weeks post-trauma was associated with a greater increase in *r*.

Sensitivity ROI and whole-brain analyses correcting for age, sex, trauma type and severity and childhood trauma are presented in Supplementary Materials and Supplementary Table 8.

Reminder acceptance. Static and dynamic reminder acceptance was predicted by lower 2-week hippocampal reactivity to social threat cues (Fig. 3a and Supplementary Materials 8). There were no statistically significant predictors in the reward or inhibition tasks. There were no statistically significant results for the whole-brain correlations between static or dynamic reminder acceptance and the inhibition, threat or reward contrasts (Table 3).

Behavioral control. Static or dynamic behavioral control did not significantly correlate with the a priori ROIs for any of the three fMRI paradigms. Whole-brain correlations with behavioral control were observed for the inhibition and reward paradigms but not threat (Fig. 3b and Table 3). During inhibition, the static behavioral control score was positively correlated with activation in the right inferior frontal gyrus (rIFG), such that greater rIFG reactivity 2 weeks post-trauma was related to greater behavioral control 6 months post-trauma. During reward processing, the static behavioral control score was negatively correlated with left precentral and postcentral gyrus activation, such that less activation was related to greater behavioral control 6 months post-trauma.

Dynamic behavioral control analyses showed positive correlations for both reward and threat processing but no associations with the inhibition task (Fig. 3b, Table 3 and Supplementary Materials 8). During reward processing, the dynamic behavioral control score positively correlated with activation in the right IPL* and right insula, such that greater activation in these regions was associated with greater increase in behavioral control from 2 weeks to 6 months post-trauma. Similarly, during threat processing, the dynamic resilience score positively correlated with activation in the bilateral IPL* and bilateral postcentral gyrus* and left precentral gyrus, such that greater threat reactivity in these regions was correlated with a greater increase in behavioral control.

https://doi.org/10.1038/s44220-024-00242-0

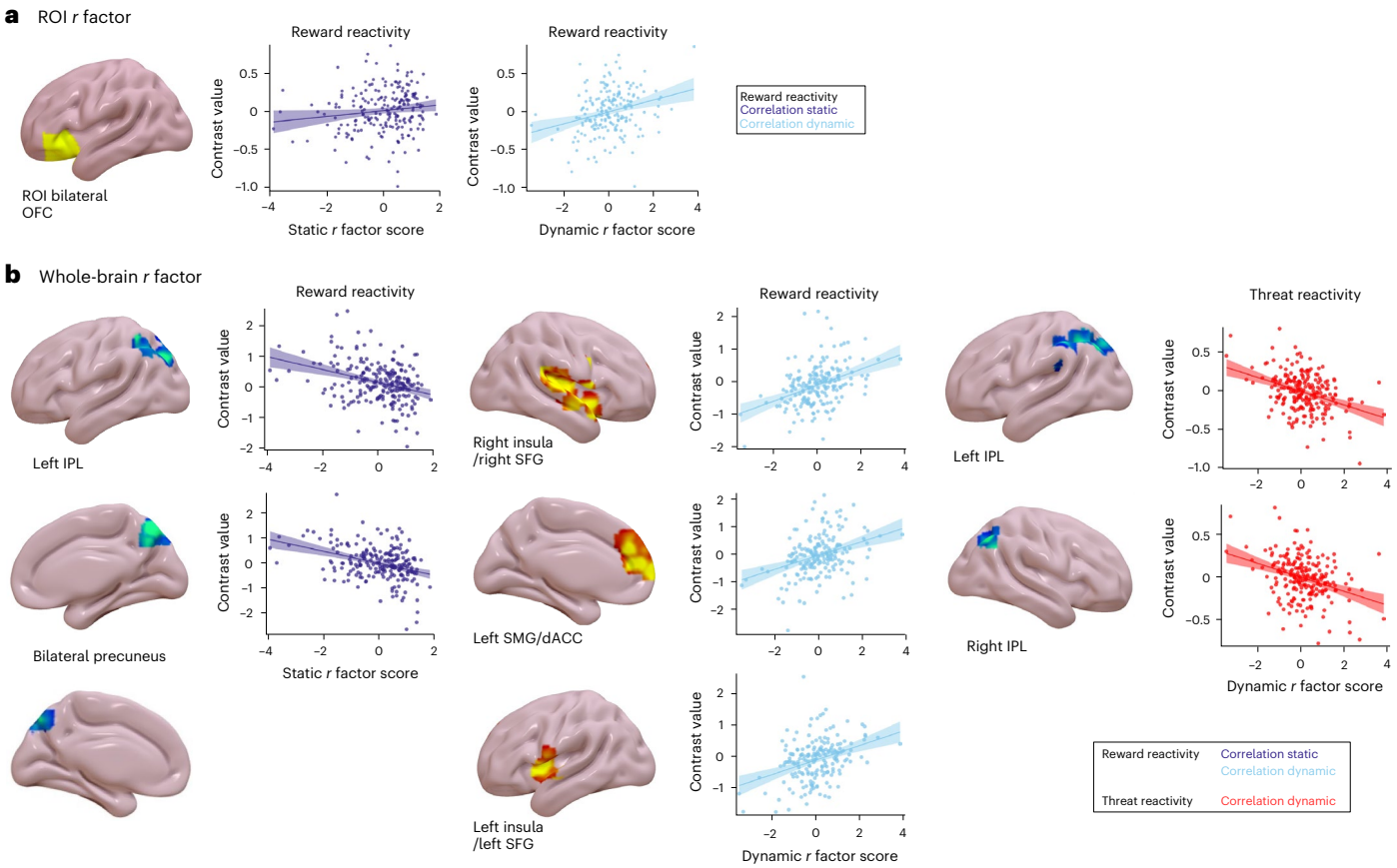

Fig. 2 | Neuroimaging correlates of the r factor. a, The results for the ROI correlation analyses with *r* factor scores. Partial correlation analyses between each ROI and static and dynamic resilience scores were performed while correcting for site using dummy variables. A significance level of $P < 0.05$ (two tailed) was used. Additional Bonferroni correction for multiple comparisons (nine ROIs, three resilience components and static and dynamic resilience, 54 tests; $P < 0.0009$) was applied, and correlations that survived this strict correction were indicated in the results section by an asterisk. The OFC ROI (top left), its correlation with the static *r* factor (purple, top middle) and correlation with the dynamic r factor (blue, top right) are depicted. Greater 2-week OFC reactivity to monetary reward (the contrast value for gain is greater than loss) 2 weeks post-trauma predicted resilience 6 months post-trauma (static *r* factor, $r = 0.14$, $P = 0.042$) and a greater increase in resilience from 2 weeks to 6 months post-trauma (dynamic *r* factor, r = 0.27, $P = 0.00015$*). The error bands indicate the 95% confidence interval. Sensitivity analyses were performed correcting for age, sex, trauma type, trauma severity and childhood trauma and correlations remained significant for the OFC (see Supplementary Materials 8 for details). **b,** Whole-brain correlations ($P < 0.005$, two sided, FWE-cluster corrected, additional Bonferroni correction for multiple comparisons across the three task domains, three components and static and dynamic resilience; 18 tests; $P < 0.0028$) with the *r* factor scores. Bottom left: the whole-brain correlations for static *r* factor scores with reactivity to monetary reward in the bilateral precuneus of the IPL. Bottom middle: the whole-brain correlations for dynamic *r* factor scores with reward-related reactivity in the left SFG right insula, left SMG, dACC, left SFG and left insula. Bottom right: the whole-brain correlations for dynamic *r* factor scores with threat-related reactivity (the contrast value for fearful is greater than the neutral faces) in the left and right IPL. The scatterplots are visual representations of the significant clusters extracted using REX for reward-related reactivity (purple for correlation static and blue for dynamic) and threat-related reactivity (red for correlation dynamic). The error bands indicate the 95% confidence interval. The sensitivity analyses were performed and the correlations remained significant ($P < 0.001$) after correcting for age, sex, trauma type, trauma severity and childhood trauma using the extracted data (see Supplementary Materials 8 for details).

Sensitivity ROI and whole-brain analyses correcting for age, sex, trauma type and severity and childhood trauma are presented in Supplementary Materials and Table 8.

Discussion

In this study, we identified a common factor for resilience that encompasses the early aftermath of trauma and assessed its functional neurobiological profile in a large longitudinal study with civilians with recent trauma exposure. We identified a main *r* factor that explained more than half of the variance across domains of mental well-being 6 months following trauma when resilient and high-groups diverge. A dynamic *r* factor was defined to account for the dynamic nature of resilience and represents recovery from initial symptoms after trauma. Two additional unique components of resilience were identified, one for reminder acceptance and one for behavioral control. These components represent small but important variance in resilience to transdiagnostic symptoms and behaviors. This study is not conclusive in the picture of resilience but highlights that different brain mechanisms may contribute to different forms of resilience. The findings highlight both a primary 'bounce back' factor primarily associated with individual differences in early poststress reward processing and additional unique aspects of resilience each subserved by a different profile of neural activity. The results serve to redefine the concept of resilience as both dynamic and multifaceted, using the large and unique post-trauma dataset we collected as part of the AURORA study. The discoveries from this investigation now generate new hypotheses and suggest novel directions for basic and clinical research.

Most individuals had a positive *r* factor score in line with the data that most people show resilience after a traumatic experience, and a positive correlation with trait resilience and negative impact of childhood trauma on the resilience score further validate the factor as a resilience-related phenotype. The assessment of early

https://doi.org/10.1038/s44220-024-00242-0

Table 3 | Correlations between *r* factors and whole-brain responses during inhibition (*n*=215), threat (*n*=249) and reward processing (*n*=214)

Component	Feature	Direction	Domain			Statistics#			MNI coordinates peak		
			Inhibition	Threat	Reward	*P* value	Cluster size	*z* score	*x*	*y*	*z*
***r* factor**	Static	Positive	–	–	Right STG	0.040	157	4.22	44	−18	−2
					Right insula	0.007	151	4.06	38	26	6
		Negative	–	–	**Bilateral precuneus**	<0.001*	376	5.09	12	−68	50
					Left IPL	0.001*	307	4.73	−38	−56	50
	Dynamic	Positive	–	–	**Right SFG. right Insula**	<0.001*	896	4.99	42	−18	0
					Left SMG, left dACC	<0.001*	353	4.89	−6	64	8
					Left SFG, left insula	<0.001*	327	4.31	−46	−2	−2
					Bilateral dACC	0.041	159	3.91	2	14	34
		Negative	–	**Left IPL**	–	<0.001*	479	5.31	−34	−72	50
				Right IPL		0.001*	341	4.44	44	−66	46
Reminder acceptance	Static/dynamic	Positive	–	–	–						
		Negative	–	–	–						
Behavioral control	Static	Positive	rIFG	–	–	0.031	179	4.28	40	12	36
		Negative	–	–	Left precentral and postcentral gyrus	0.003	246	3.87	−68	−14	22
	Dynamic	Positive	–	**Right postcentral gyrus right IPL**		0.001*	357	4.37	56	−26	46
				Left precentral gyrus		0.003	293	4.57	−56	14	30
				Left IPL left postcentral gyus		0.005	268	3.76	−56	−22	40
					Right IPL	<0.001*	471	4.08	44	−46	44
					Right insula	0.010	205	4.27	38	24	−2
		Negative	–	–	–						

#Whole-brain level partial correlation analyses were conducted using a primary threshold $P<0.005$ and cluster-level FWE-corrected threshold ($P<0.05$, two sided). The cluster-level FWE-corrected *P* values and corresponding cluster size are reported. The *z* score for the peak voxel and corresponding Montreal Neurological Institute (MNI) coordinates are reported. Starred *P* values and the bolded regions indicate clusters that survived additional Bonferroni correction for three domains (tasks), the three components (*r* factor, reminder acceptance and behavioral control) and two features (static and dynamic), 18 tests, $P<0.0028$. Exact *P* values are included in Supplementary Table 8b.

post-trauma neuroimaging predictors of the *r* factor across inhibition, threat and reward-related domains showed a dominant role of reward processing in explaining global stress resilience. The response to monetary reward within the OFC, a regulatory structure implicated in encoding value and central to reward processing[20,21], was positively related to static and dynamic features of global stress resilience, though only the association with dynamic resilience survived Bonferroni correction ($P < 0.0009$). Greater reward-related activation in the insula also predicted greater resilience. The role of the insula in interoceptive awareness and subjective emotional experiences is key in the salience network for directing attention to salient stimuli[22]. Positive correlations were also observed with the dACC and bilateral SFG, regions for higher cognitive functioning and control, and decision-making based on social or reward-related information[23–27]. Together the insula, dACC and SFG make up components of the cingulo-opercular 'action mode network'[28], which is theorized to work in opposition to the default mode network, supporting a dampening of default processes, heightened alertness and an external focus. These neuroimaging findings suggest that greater prefrontal guidance in the use of emotional and salient information for decision-making and interoceptive awareness and attention to reward (versus loss) promotes global stress resilience, which represents a validation and functional converse of two meta-analyses on common neuroimaging markers for transdiagnostic psychopathology irrespective of trauma[29,30].

Conversely, lower activation in the bilateral precuneus and left posterior IPL during reward processing was associated with greater resilience. Precuneus and posterior IPL are key nodes of the (posterior) default mode network and implicated in internally generated attention and critical regions for spatial attention[31–34]. It is postulated that attention from these top-down sources competes with bottom-up sources using (reward) salience (that is, insula, ACC and OFC) to affect decision-making[35]. Prior studies show that the engagement of similar top-down attention neurocircuitry slows down the search for salient targets[36], and our findings imply that resilience is hampered by the engagement of regions within the top-down attention or default mode network to reward or threat cues but benefits from attention to reward salience and regulatory control of higher order brain regions. It is important to distinguish the immediate reward processing, which we measured here, from longer-term reward processing, such as delay discounting, that could show different patterns. Potential therapeutic interventions building on our immediate reward processing findings

https://doi.org/10.1038/s44220-024-00242-0

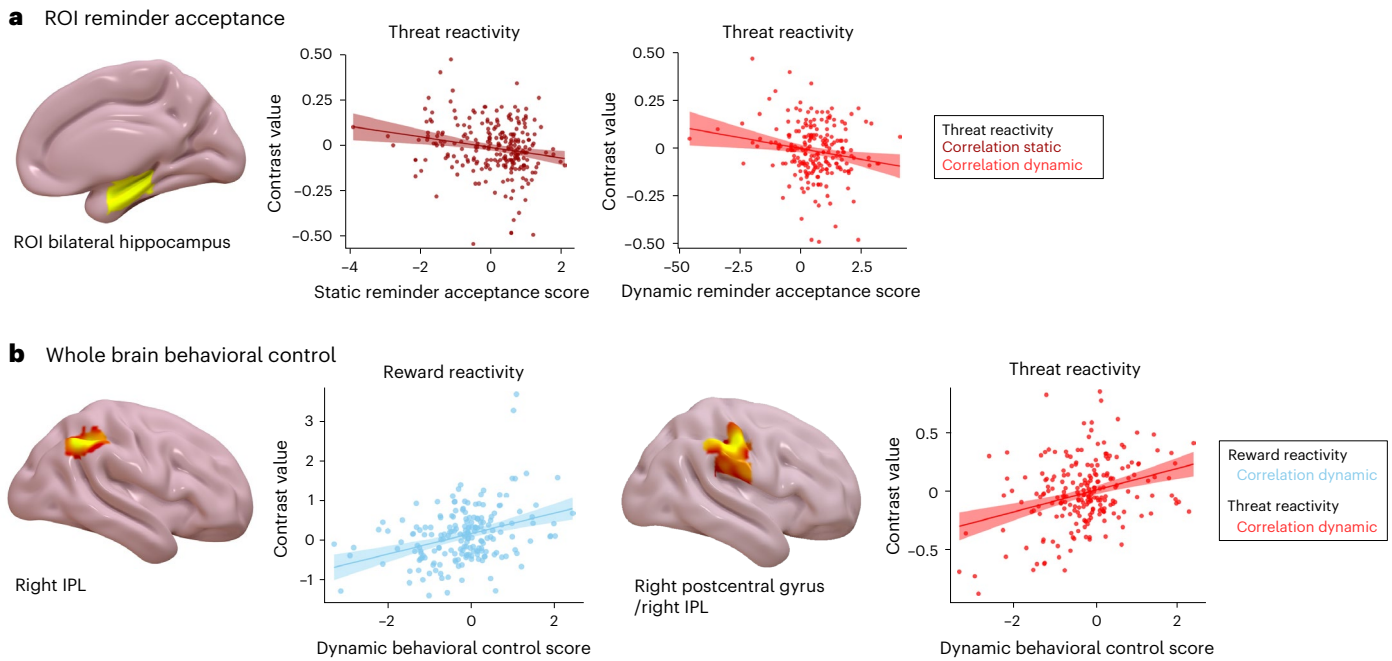

Fig. 3 | Neuroimaging correlates of reminder acceptance and behavioral control. a, The results for the ROI correlation analyses with reminder acceptance scores. Partial correlation analyses between each ROI and static and dynamic scores were performed while correcting for site using dummy variables. A significance level of $P < 0.05$ (two tailed) was used. Additional Bonferroni correction for multiple comparisons (nine ROIs, three resilience components and static and dynamic resilience, 54 tests; $P < 0.0009$) was applied, and correlations that survived this strict correction were indicated in the results section by an asterisk. The bilateral hippocampus ROI (top left), its correlation with static reminder acceptance (dark red, top middle) and the correlation with dynamic reminder acceptance (red, top right) are depicted. A lower 2-week hippocampal reactivity to threat cues (the contrast value for fearful is greater than the neutral faces) predicted greater reminder acceptance 6 months post-trauma (static reminder acceptance, $r = -0.20$, $P = 0.002$) and a greater increase in reminder acceptance from 2 weeks to 6 months post-trauma (dynamic reminder acceptance, $r = -0.17$, $P = 0.012$). The error bands indicate the 95% confidence interval. Sensitivity analyses were performed correcting for age, sex, trauma type, trauma severity and childhood trauma. The correlations remained significant but did not survive Bonferroni correction (see Supplementary Materials 8 for details). **b,** Whole-brain correlations ($P < 0.005$, two sided, FWE-cluster corrected, additional Bonferroni correction for multiple comparisons across the three task domains, three resilience components and static and dynamic features; 18 tests; $P < 0.0028$) for dynamic behavioral control. Bottom left: the significant correlation for behavioral control with reactivity to monetary reward (the contrast value for gain is greater than loss) in the right IPL. Bottom right: the significant correlation for behavioral control with threat-related reactivity in the right postcentral gyrus. The scatterplot is a visual representation of the significant cluster that was extracted using REX for reward processing (blue) and threat processing (red). The error bands indicate the 95% confidence interval. The sensitivity analyses were performed and correlations remained significant ($P < 0.001$) after correcting for age, sex, trauma type, trauma severity and childhood trauma using the extracted data (see Supplementary Materials 8 for details).

could include attention bias training focusing on positive, rewarding cues to guide behavior. Indeed, positive attention bias training improved mental health in children and adolescents[37], supporting the notion that attentional bias to positive and not to threat-related stimuli promotes resilience. Targeted brain stimulation to engage the superior frontal and medial gyrus in individuals at risk could be another interesting approach to consider after further study of this association, though more precision is needed before this can be operationalized.

Two secondary components of resilience for reminder acceptance and behavioral control were identified in this study. Lower threat-related hippocampal activation correlated with greater (increase of) resilience to trauma reminders, though this finding did not survive Bonferroni correction, and the result should be interpreted with caution. The hippocampus has consistently been implicated in PTSD and (trait) resilience, though direction of findings have been varied[6,7,38–40], possibly because subregions of the hippocampus are typically pooled together in one ROI regardless of their unique functions and different functional connectivity, for example identified in PTSD[41]. Furthermore, type of symptoms could differentiate hippocampal involvement. Reexperiencing symptoms has been associated with overengagement of the hippocampus during emotional memory encodings[42], whereas more distress-related symptoms are associated with poorer engagement of hippocampal memory, which is in line with our earlier publication showing lower hippocampal activation in participants with PTSD symptoms at 2 weeks[43]. Our results, therefore, suggest the importance of exploring multiple dimensions of resilience that could explain prior disagreements in the research for which dimensions were mixed.

Behavioral control was not well-captured by the a priori ROIs but instead showed strong associations with a variety of inhibition-related regions across all three fMRI tasks. The most robust finding was greater right IPL reactivity to threat and reward predicting greater recovery of behavioral control over time. The significant cluster for behavioral control included the postcentral gyrus and was anterior to the IPL region observed for the *r* factor. In addition to its role as part of the DMN, the more anterior parts of the IPL have been implicated in inhibitory control[44,45], which could explain its association with behavioral control. Prior studies showed that greater IPL reactivity predicted greater recovery from PTSD[45], whereas lower IPL activation was associated with greater impulsive behavior in problem gamers[46] and the impulsive subtype of attention-deficit/hyperactivity disorder[47]. We similarly demonstrated that greater inhibition-related rIFG activation during the inhibition task was associated with greater behavioral control at 6 months. The rIFG is another key region for inhibition and impulse control, and though this finding was not robust to the additional Bonferroni correction for multiple testing, it supports earlier findings of lower inhibition-related rIFG activation in PTSD[48,49], alcohol craving and drinking[50] and change in response with age[51].

Prior studies investigating the neurobiology of resilience generally concluded that lower threat reactivity in the amygdala and greater activation in prefrontal, hippocampal and salience network regions were associated with greater levels of resilience mostly using threat- or inhibition-related paradigms[3]. Few studies in the early aftermath of trauma have investigated reward-related processing[52–54], and the current study shows the importance of studying neurobiological mechanisms of reward processing in addition to threat and inhibition. A second limitation of prior research includes small sample sizes and limited power for unbiased (whole-brain) analyses. Indeed, most studies used ROI analyses and focused on brain regions of the threat neurocircuitry (including the amygdala, hippocampus and vmPFC), whereas our whole-brain analyses suggest important associations with cortical regions outside previously studied regions and providing new directions for future study and interventions.

One important limitation of our study is that scans were collected 2 weeks post-trauma, and brain responses possibly or partly represent adaptations in this early post-trauma period. We addressed the possibility of early changes by including 2-week data in the dynamic analyses. Further, we are interested in mechanisms of change from this 2-week time point, as this early period following trauma may provide the best window of opportunity for early interventions in a civilian population. Nevertheless, true prospective studies, such as a notable one in ref. 4, investigate different mechanisms, and therefore our conclusions cannot be generalized to all time points given the dynamics of resilience. It is also important to note that our dynamic *r* factor captures the change from early symptoms following trauma and future directions include a deeper dive into the dynamic scores by evaluating more detailed time courses of fluctuation in symptoms. Moreover, it does not capture dynamics in resilience that could change with repeated trauma or other forms of stress. Lifetime trauma exposure influences our resilience scores, and it is important to recognize that our *r* factor score reflects a combination of variables (including biological sex, age and childhood trauma) that contribute to mental well-being following recent trauma exposure. An important strength of our study is that all participants have recently experienced a traumatic event (mostly motor vehicle collisions), and our approach is most productive for the development of early interventions. Additionally, the test–retest reliability for the three fMRI tasks used in this investigation is unknown. This is an important limitation given recent substantial critiques of the within-subjects reliability that is possible to obtain using many well-studied fMRI tasks[55]. We apply Bonferroni corrections for our ROI analyses ($P < 0.0009$) to promote reproducibility of our findings, but our power analyses suggest we may be underpowered to detect effects in our ROIs with this stringent correction. Another limitation is that the results are not yet externally replicated and an earlier replication attempt of the AURORA study was not successful[56], suggesting it would be important to see if similar patterns arise in a different dataset before, for example, moving to targeted neuromodulation of regions implicated here.

Conclusion

In this large study on civilians with recent trauma exposure, we identify a common factor for resilience, the *r* factor, that explains more than half the variance of mental well-being in the first 6 months following trauma exposure. Our definition of the *r* factor and its neural correlates is not conclusive but instead provides important novel insights into the structure of mental well-being after trauma exposure and may accelerate research on resilience and novel early interventions following trauma. These findings provide interesting new directions for resilience research including the use of a common factor across domains and investigating reward processing as a central construct for resiliency.

Methods

Inclusion and ethics statement

The research complies with all relevant ethical regulations. The institutional review board (IRB) of the University of North Carolina approved the study protocol (IRB no. 1707-03) as a multisite human subject study on 12 May 2017, and other sites created either reliance agreements or parallel IRBs. The data analyses were conducted at Emory University, and the local IRB number is IRB00097424. All participants provided written informed consent. An independent medical study monitor reviewed and approved the standard operating procedures associated with evaluating and managing individuals reporting clinical worsening or as identified by study personnel. The monitor also reviewed written reports detailing participant contacts by experienced clinicians.

Participants

The participants were recruited as part of the multisite ED AURORA study[16]. The participants with trauma exposure, defined for this study as a traumatic event requiring evaluation at an ED, were approached within 72 h of their event. This study sample of participants in the early aftermath of trauma was chosen to investigate critical changes in neurobiology and brain function that increase the risk for trauma-related psychopathology in the weeks or months after trauma. The goal was to enroll a sample representative of the US population, and there were no enrollment restrictions with regards to demographic variables including sex or gender and race or ethnicity. Participants were compensated $60 for enrollment and initial evaluation, $100 (total) for the 2-week and 6-month evaluations and $105 for the magnetic resonance imaging (MRI) procedure.

The participants who experienced certain traumatic events, including a motor vehicle collision, high fall (>10 ft), physical assault, sexual assault or mass casualty incidents automatically qualified for study inclusion. Other participants qualified for study inclusion after experiencing other types of trauma if: (1) the individual responded to a screener question that they experienced the traumatic exposure as involving actual or threatened serious injury, sexual violence or death, either by direct exposure, witnessing or learning about the trauma and (2) the research assistant agreed that the traumatic exposure involved actual or threatened serious injury, sexual violence or death and was therefore a plausible qualifying event. This investigation included $n = 2{,}772$ AURORA participants with clinical item-level data at 2 weeks or 6 months recruited from September 2017 to December 2020 (final freeze for psychometric release). The missing data values were excluded listwise, resulting in $n = 1{,}835$ (1,175 women; Table 1) participants with complete 6-month item-level clinical data usable for analyses.

The participants recruited for AURORA at one of the ED sites that funneled participants to one of the five 'deep phenotyping' sites were invited to undergo an MRI scan (details in ref. 17). fMRI data were collected for $n = 445$; the fMRI scan included a response inhibition paradigm ($n = 428$), a fearful faces 'social threat' task ($n = 431$) and a monetary reward processing task ($n = 427$). Functional data were excluded from analyses for anatomical concerns ($n = 7$), lack of expected behavioral responses or available data ($n = 45$ for inhibition, $n = 14$ for threat processing and $n = 26$ for reward processing), excessive motion (any run with greater than 15% of volumes exceeding 1 mm framewise displacement; inhibition, $n = 33$; threat, $n = 25$; reward, $n = 45$) or technical issues during the scan ($n = 14$ for inhibition, $n = 15$ for threat processing and $n = 24$ for reward processing). The final data were available for $n = 385$ for at least one of the tasks ($n = 329$ for inhibition, $n = 370$ for threat processing and $n = 325$ for reward processing). Of these, associations with resilience scores were investigated for $n = 260$ individuals who had scores available ($n = 215$ for inhibition, $n = 249$ for threat processing and $n = 214$ for reward processing; Table 1). Dynamic resilience scores (both complete 2-week and 6-month clinical data) were investigated for, respectively, $n = 189$, $n = 221$ and $n = 189$. Both a priori and post hoc power analyses were computed (Supplementary Methods and Supplementary Tables 1 and 2).

Demographic and clinical data collection

The ED assessments were conducted by trained research assistants. There were no restrictions to the presence of other individuals

including hospital personnel or family members or friends. There were no experimental conditions or specific study hypotheses, but the research assistants were aware of the general study goals. The participants completed interview and self-administered surveys in the ED. The participants also had the Mindstrong Discovery Android/iOS smartphone app (iOS version 2.2; Android version 1.5.1) downloaded onto their smartphone. The follow-up surveys were completed 2 weeks, 8 weeks, 3 months, 6 months and 12 months after initial evaluation via web-based or phone assessments via self-report surveys. For this manuscript, data collected in the ED at 2 weeks and 6 months following trauma exposure were used in accordance with prior work showing at 6 months resilience and high-risk groups diverge[15], and the 2-week time point represents the peritrauma period and corresponds with the time point of the MRI scan, thereby providing a good window to account for changes after the scan in this peritrauma period.

The demographic data were collected using self-report after enrollment in the ED and included race and Hispanic ethnicity, sex assigned at birth, marital status, income and education level and employment. Additionally, childhood abuse and neglect was assessed with the Childhood Trauma Questionnaire-Short Form (CTQ-SF)[57] and trait resilience was assessed with the Connor–Davidson Resilience Scale[58]. Trauma type was measured using a categorical variable. Trauma severity was measured with the ISS and the abbreviated injury scale (AIS)[59]. The ISS takes into account multiple injuries and regions. The AIS is an international standard tool for ranking the severity of injury on a 6-point ordinal scale. The score equals the sum of the squares of the highest AIS scores. Pain in the ED is measured with the Numeric Pain Rating Scale, and the question number of body parts with pain (0–18) was used as a continuous variable[60]. The trauma type was quantified by assigning each individual's trauma to the corresponding trauma type category, and the categories were numbered and used as categorical variable in analyses.

The item-level clinical data were collected with flash surveys at 2 weeks and 6 months post-trauma, and the raw scores for 45 items were used for the analyses (Table 2). From the Patient-Reported Outcomes Measurement Information System (PROMIS)[61,62], nine items were included for depression, four items for anxiety and two for sleep. The PROMIS items were rated on a scale from 1 (none of the time) to 5 (all or almost all the time). A total of 20 items were included from the PTSD checklist for the Diagnostic and Statistical Manual of Mental Disorders, Fifth Edition (PCL-5)[63], a well-validated questionnaire on PTSD symptom presence and severity where participants are asked to rate their symptoms on a scale from 0 (not at all) to 4 (extremely). Two items were included for number of days of alcohol use and nicotine using the PhenX Toolkit[64]. Finally, eight items from the Impulsive Behavior Scale–short form[65] were included to measure impulsive behavior using using a scale from 1 (never) to 5 (very often).

Statistics and reproducibility

The study is a quantitative longitudinal observational study. The experiments were not randomized, and the investigators were not blinded to outcome assessments. The patients who presented to the ED within 72 h of trauma exposure at participating ED sites were screened for study eligibility. The goal was to enroll 5,000 participants in the study, with adaptive sampling of specific trauma subsamples and adjustment of study design over the course of the study as necessary to achieve study goals. The study was not powered to address a specific hypothesis and, instead, given the fixed budget and multiple study aims, the study was designed to have the largest possible sample size while collecting all the types of data needed to address the aims of the parent project. The aims included identifying and characterizing trajectories of the most common trauma-induced symptoms across mental and physical health domains and to conduct machine learning to identify individuals at high risk of adverse outcomes following trauma. The study concluded in December 2020 with a final sample of $n = 2{,}943$ with follow-up data. The data for the current manuscript included participants with complete item-level 6-month follow-up data ($n = 1{,}835$). The subsamples of study participants who lived within driving distance of an AURORA neuroimaging or deep phenotyping site were asked to return for in-person evaluations 2 weeks after the ED visit ($n = 445$ total). A total of $n = 260$ were included in the neuroimaging analyses (after excluding for anatomical concerns, lack of behavioral responses or available data, excessive motion, technical issues or incomplete *r* factor data). The power analyses for neuroimaging data are included in Supplemental Materials 1.

Statistical analyses consisted of several steps, which are detailed in the sections below. In brief, the first step included PCA for resilience, which was conducted for $n = 1{,}835$ in Statistical Package for the Social Sciences (SPSS) v.28.0, and examination of the external validity of the resilience-related components by examining associations with established resiliency questionnaires, age and sex and childhood trauma exposure. Second, neuroimaging analyses for $n = 260$ were conducted starting with centralized preprocessing of fMRI data in fMRIPrep v1.1.2. The first-level neuroimaging analyses were conducted in statistical parametric mapping (SPM) 12. Then ROI analyses were conducted, extracting ROIs using REX software. The ROI correlation analyses were performed in SPSS. Finally, whole-brain analyses were conducted in SPM12. Rigorous statistical thresholds were used to promote replicability of the findings.

PCA for resilience

PCA using the item-level clinical data was performed using SPSS v28.0. Varimax rotation with a maximum of 25 iterations for convergence was used. The components were extracted based on eigenvalues greater than 2. The scores were saved as variables to create resilience scores for 6 months (static resilience scores). To create dynamic resilience scores, we estimated the 2-week resilience scores based on the loadings derived from the 6-month data created with the PCA. Time of assessment (2 weeks versus 6 months) was used as a selection variable, such that the PCA was based on 6-month data, and estimated factor scores were computed for the 2-week data using the same factors. The 2-week scores were subtracted from the 6-month static scores to calculate dynamic resilience scores. Table 2 presents the varimax rotation loadings for each of the items for each factor. These participant-level static and dynamic resilience scores were used for the neuroimaging analyses.

fMRI

High-resolution T1-weighted structural scans were collected using multiecho magnetization-prepared rapid acquisition gradient echo (MP-RAGE) using comparable parameters across the five imaging sites (site 1: repetition time (TR) of 2,530 ms; echo times (TE) of 1.74, 3.6, 5.46 and 7.32 ms; inversion time (TI) of 1,260 ms; flip angle of 7; field of view (FOV) of 256 mm; 176 slices; and voxel size of 1 mm × 1 mm × 1 mm. Site 2: TR of 2,530 ms; TEs of 1.74, 3.6, 5.46 and 7.32 ms; TI of 1,260 ms; flip angle of 7, FOV 256 mm, 176 slices; and voxel size of 1 mm × 1 mm × 1 mm. Site 3: TR of 2,300 ms, TE of 2.96 ms, TI of 900 ms, flip angle of 9, FOV of 256 mm, 176 slices, and voxel size of 1.2 mm × 1.0 mm × 1.2 mm. Site 4: TR of 2,530 ms; TEs of 1.74, 3.65, 5.51 and 7.72 ms; TI of 1,260 ms; flip angle of 7, FOV of 256 mm; 176 slices; and voxel size of 1 mm × 1 mm × 1 mm. Site 5: TR of 2,300 ms, TE of 2.98 ms, TI of 900 ms, flip angle of 9, FOV of 256 mm, 176 slices, and voxel size of 1.2 mm × 1.0 mm × 1.2 mm). One imaging site collected a standard 1-mm isotropic MP-RAGE sequence, as it was unable to collect MP-RAGE scans. fMRI data were collected using identical parameters to measure blood-oxygen-level-dependent signals across sites; however, scan time slightly different between sites (site 1: TR of 2,360 ms, TE of 30 ms, flip angle of 70, FOV of 212 mm, 44 slices, voxel size of 3 mm × 2.72 mm × 2.72 mm and 0.5 mm gap; site 2: TR of 2,360 ms, TE of 30 ms, flip angle of 70, FOV of 212 mm, 44 slices, voxel size of 3 mm × 3 mm × 3 mm and 0.5 mm gap; site 3: TR of 2,360 ms, TE of 29 ms, flip angle of 70, FOV of 212 mm, 44 slices, voxel size of 3 mm × 2.72 mm × 2.72 mm and 0.5 mm gap; site 4: TR

of 2,360 ms, TE of 30 ms, flip angle of 70, FOV of 212 mm, 42 slices, voxel size of 3 mm × 2.72 mm × 2.72 mm and 0.5 mm gap; site 5: TR of 2,360 ms, TE of 29 ms, flip angle of 90, FOV of 210 mm, 44 slices, voxel size of 3 mm × 3 mm × 2.5 mm and 0.5 mm gap). See Supplementary Table 7 for details. The site was included as a covariate (using dummy variables) in all neuroimaging analyses.

fMRI was performed during presentation of three functional tasks to assess inhibition, threat and reward processes, also described in a prior publication[17]. The three task paradigms were selected for the AURORA study because they have consistently been shown to activate neural substrates of interest and represent the National Institutes of Health (NIH) Research Domain Criteria domains. Inhibition was measured using the Go/NoGo task[55]. The participants were shown either an X or an O for 1,000 ms and were instructed to press 1 for X and 2 for O (Go trials) but not press a button when a red rectangle appeared behind the X or the O (NoGo trial). The task consists of four runs with 26 Go trials, 13 NoGo trials and 14 blank trials consisting of a black background only. The trials were presented in random order. The trials were followed by a jittered intertrial interval of 1,250–2,500 ms and a 500 ms fixation cross. Threat processing was assessed with the fearful faces task[66]. The participants viewed blocks of static fearful and neutral faces from the Ekman and Friesen faces library. A total of 15 blocks with fearful faces and 15 blocks with neutral faces were presented in pseudorandom order, and the block order was counterbalanced across participants. Each 6,000-ms block consisted of eight different face simuli, each presented for 500 ms with a 500 ms interstimulus interval. After every ten blocks, a 10,000 ms rest period occurred in which the participants were instructed to relax. For reward processing, a short version of Delgado's monetary reward task[67] was used. The participants viewed a card with a question mark and were asked to indicate by a button press whether they guess the card's value would be higher or lower than 5 before the real value was revealed. A total of 40 trials were presented, each including a 2,000-ms guessing period in which a button press was recorded, then the card's value and monetary outcome was presented after a 2,000–4,000 ms delay. The participants were told they would win $1 for each correct guess and lose $0.50 for each incorrect guess and were told they would receive this money. Unknown to the participants, the outcome was predetermined to create ten wins and ten losses, resulting in $10.

Preprocessing information is reported in detail in our prior study[17]. Briefly, the functional images were preprocessed with fMRIPrep, version 1.2.2 (ref. 18). Echo-planar imaging scans were coregistered to the T1-weighted images. The scans were spatially realigned, slice-time corrected and normalized to the 2009 International Consortium for Brain Mapping-152 template. Independent Component Analysis-based Automatic Removal of Motion Artifacts was used to correct for volume-wise motion and other sources of artifact[68]. An overall motion threshold was implemented for any run with greater than 15% of volumes with more than a 1 mm framewise displacement to handle cases in which motion was probably too high for effective Independent Component Analysis correction. Finally, the images were smoothed with a 6-mm kernel.

First-level statistical modeling was conducted in SPM12. For the Go/NoGo task, correct Go and correct NoGo trials were modeled in an event-related design (0 ms event duration), and incorrect Go and NoGo trials were modeled separately. The contrast of correct NoGo>Go trials was used to measure response inhibition. For the fearful faces task, blocks of fearful and neutral stimuli were modeled with separate boxcar functions representing the onset and 8,000 ms duration of each block and were convolved with a canonical hemodynamic response function. The fearful>neutral face contrast was used to measure threat processing. For the card task, the gain and loss trials were modeled as separate experimental conditions in an event-related design. Furthermore, each trial during which the participant did not press a button was modeled in an error condition. The gain>loss contrast was used to measure reward processing. In all first-level models, nuisance regressors included white matter, cerebrospinal fluid and global signal time courses.

ROI analyses

ROIs were selected for the larger AURORA study[17] and consistently used here. Anatomical boundaries were used to define bilateral ROIs. For inhibition (NoGo>Go contrast), the hippocampus (Hammers atlas[69]) and the vmPFC (defined based on our prior study findings; 6-mm sphere around −4, 44, −4 (ref. 70)) were used. For threat processing (fearful>neutral faces contrast), the amygdala (based on the CITI168 subcortical atlas[71]), the bilateral hippocampus (Hammers atlas) and the subgenual anterior cingulate cortex (sgACC) and dACC, respectively, defined ad BA25 and BA32 (map of the Brodmann area from the WFUPickAtlas), were used. For reward processing (gain>loss), the nucleus accumbens and bilateral amygdala (CITI168 subcortical atlas) and OFC (Harvard–Oxford atlas) were used. The mean across all voxels in each ROI was extracted from first-level contrasts using REX[19], also described in our earlier papers[43,66].

To test our hypotheses that greater ROI contrast values were related to greater static and dynamic resilience scores, partial correlation analyses between each ROI and static and dynamic resilience scores were performed while correcting for site using dummy variables. The outliers with contrast values that deviated more than three standard deviations (s.d.) from the mean were assessed and excluded separately per task ($n = 2$ for inhibition, $n = 5$ for threat processing and $n = 2$ for reward processing). A significance level of $P < 0.05$ (two tailed) was used. Additional Bonferroni correction for multiple comparisons (nine ROIs, three resilience components and static and dynamic resilience, 54 tests; $P < 0.0009$) was applied, and correlations that survived this strict correction were indicated in the results section by an asterisk.

Whole-brain analyses

Whole-brain group-level maps were created for inhibition, threat and reward contrasts and included dummy variables for site. A factorial design with multiple regressors was used to examine the voxel-level correlations between the contrast estimates for inhibition, threat and reward with each of the continuous resilience scores as covariates in separate models. A primary threshold of $P < 0.005$ combined with a family wise error (FWE) cluster-level correction was applied to correct for multiple comparisons using the default in SPM12. Clusters surviving the FWE-corrected threshold are reported in Table 3. Additional Bonferroni correction was applied to correct for the three task domains, three components and static and dynamic resilience (18 tests, $P < 0.0028$; indicated by an asterisk in Table 3). The means of the clusters robust to the additional Bonferroni correction were extracted and are displayed in Figs. 2 and 3.

Reporting summary

Further information on research design is available in the Nature Portfolio Reporting Summary linked to this article.

Data availability

We agree to make materials, data and associated protocols promptly available without undue qualifications. The data and/or research tools used in the preparation of this manuscript were obtained from the NDA. The NDA is a collaborative informatics system created by the NIH to provide a national resource to support and accelerate research in mental health. The dataset identifier(s) include the NIMH Data Archive digital object identifier 10.15154/zwyn-rb26. The masks used for the ROI analyses are freely available. The Hammers atlas is available via https://brain-development.org/brain-atlases/ (ref. 72), the CITI168 subcortical atlas via https://osf.io/r2hvk/wiki/home/ (ref. 73), the WFUPickAtlas via https://www.nitrc.org/projects/wfu_pickatlas (ref. 74) and the Harvard/Oxford atlas via https://neurovault.org/collections/262/ (ref. 75). REX software is available via https://www.nitrc.org/projects/rex/ (ref. 19).

Code availability

We agree to make code promptly available without undue qualifications. More information is available at https://github.com/sjhvanrooij/rfactor (ref. 76).

References

1. Resilience definition and meaning. *Merriam-Webster* https://www.merriam-webster.com/dictionary/resilience
2. Kalisch, R. et al. Deconstructing and reconstructing resilience: a dynamic network approach. *Perspect. Psychol. Sci. J. Assoc. Psychol. Sci.* **14**, 765–777 (2019).
3. Roeckner, A. R., Oliver, K. I., Lebois, L. A. M., van Rooij, S. J. H. & Stevens, J. S. Neural contributors to trauma resilience: a review of longitudinal neuroimaging studies. *Transl. Psychiatry* **11**, 508 (2021).
4. Kaldewaij, R. et al. Anterior prefrontal brain activity during emotion control predicts resilience to post-traumatic stress symptoms. *Nat. Hum. Behav.* **5**, 1055–1064 (2021).
5. Richter, A., Krämer, B., Diekhof, E. K. & Gruber, O. Resilience to adversity is associated with increased activity and connectivity in the VTA and hippocampus. *NeuroImage Clin.* **23**, 101920 (2019).
6. van Rooij, S. J. H. et al. Childhood trauma and COMT genotype interact to increase hippocampal activation in resilient individuals. *Front. Psychiatry* **7**, 156 (2016).
7. van Rooij, S. J. H. et al. Hippocampal activation during contextual fear inhibition related to resilience in the early aftermath of trauma. *Behav. Brain Res.* **408**, 113282 (2021).
8. Luthar, S. S. & Brown, P. J. Maximizing resilience through diverse levels of inquiry: prevailing paradigms, possibilities, and priorities for the future. *Dev. Psychopathol.* **19**, 931–955 (2007).
9. Luthar, S. S., Cicchetti, D. & Becker, B. The construct of resilience: a critical evaluation and guidelines for future work. *Child Dev.* **71**, 543–562 (2000).
10. Rutter, M. Resilience: some conceptual considerations. *J. Adolesc. Health* **14**, 626–631 (1993).
11. Wallbrown, F. H., Blaha, J., Wallbrown, J. D. & Engin, A. W. The hierarchical factor structure of the wechsler intelligence scale for children-revised. *J. Psychol.* **89**, 223–235 (1975).
12. Caspi, A. et al. The *p* factor: one general psychopathology factor in the structure of psychiatric disorders? *Clin. Psychol. Sci. J. Assoc. Psychol. Sci.* **2**, 119–137 (2014).
13. Caspi, A. & Moffitt, T. E. All for one and one for all: mental disorders in one dimension. *Am. J. Psychiatry* **175**, 831–844 (2018).
14. van Harmelen, A.-L. et al. Adolescent friendships predict later resilient functioning across psychosocial domains in a healthy community cohort. *Psychol. Med.* **47**, 2312–2322 (2017).
15. Galatzer-Levy, I. R. et al. Early PTSD symptom trajectories: persistence, recovery, and response to treatment: results from the jerusalem trauma outreach and prevention study (J-TOPS). *PLoS ONE* **8**, e70084 (2013).
16. McLean, S. A. et al. The AURORA Study: a longitudinal, multimodal library of brain biology and function after traumatic stress exposure. *Mol. Psychiatry* **25**, 283–296 (2020).
17. Stevens, J. S. et al. Brain-based biotypes of psychiatric vulnerability in the acute aftermath of trauma. *Am. J. Psychiatry* **178**, 1037–1049 (2021).
18. Esteban, O. et al. fMRIPrep: a robust preprocessing pipeline for functional MRI. *Nat. Methods* **16**, 111–116 (2019).
19. REX. *NITRIC* https://www.nitrc.org/projects/rex/ (2007).
20. O'Doherty, J., Kringelbach, M. L., Rolls, E. T., Hornak, J. & Andrews, C. Abstract reward and punishment representations in the human orbitofrontal cortex. *Nat. Neurosci.* **4**, 95–102 (2001).
21. Wallis, J. D. & Kennerley, S. W. Contrasting reward signals in the orbitofrontal cortex and anterior cingulate cortex. *Ann. N. Y. Acad. Sci.* **1239**, 33–42 (2011).
22. Menon, V. & Uddin, L. Q. Saliency, switching, attention and control: a network model of insula function. *Brain Struct. Funct.* **214**, 655–667 (2010).
23. Hu, S., Ide, J. S., Zhang, S. & Li, C.-S. R. The right superior frontal gyrus and individual variation in proactive control of impulsive response. *J. Neurosci. Off. J. Soc. Neurosci.* **36**, 12688–12696 (2016).
24. du Boisgueheneuc, F. et al. Functions of the left superior frontal gyrus in humans: a lesion study. *Brain J. Neurol.* **129**, 3315–3328 (2006).
25. Brockett, A. T., Tennyson, S. S., deBettencourt, C. A., Gaye, F. & Roesch, M. R. Anterior cingulate cortex is necessary for adaptation of action plans. *Proc. Natl Acad. Sci. USA* **117**, 6196–6204 (2020).
26. Doya, K. Modulators of decision making. *Nat. Neurosci.* **11**, 410–416 (2008).
27. Behrens, T. E. J., Hunt, L. T., Woolrich, M. W. & Rushworth, M. F. S. Associative learning of social value. *Nature* **456**, 245–249 (2008).
28. Dosenbach, N. U. F., Raichle, M. & Gordon, E. M. The brain's cingulo-opercular action-mode network. Preprint at *PsyArXiv* https://doi.org/10.31234/osf.io/2vt79 (2024).
29. Goodkind, M. et al. Identification of a common neurobiological substrate for mental illness. *JAMA Psychiatry* **72**, 305–315 (2015).
30. McTeague, L. M. et al. Identification of common neural circuit disruptions in emotional processing across psychiatric disorders. *Am. J. Psychiatry* **177**, 411–421 (2020).
31. Mahayana, I. T., Tcheang, L., Chen, C.-Y., Juan, C.-H. & Muggleton, N. G. The precuneus and visuospatial attention in near and far space: a transcranial magnetic stimulation study. *Brain Stimul.* **7**, 673–679 (2014).
32. Lee, J. et al. rTMS over bilateral inferior parietal cortex induces decrement of spatial sustained attention. *Front. Hum. Neurosci.* **7**, 26 (2013).
33. Hommet, C. et al. Unilateral spatial neglect following right inferior parietal cortectomy. *Epilepsy Behav.* **5**, 416–419 (2004).
34. Smallwood, J. et al. The default mode network in cognition: a topographical perspective. *Nat. Rev. Neurosci.* **22**, 503–513 (2021).
35. Zhang, W., Xie, Y. & Yang, T. Reward salience but not spatial attention dominates the value representation in the orbitofrontal cortex. *Nat. Commun.* **13**, 6306 (2022).
36. Anderson, B. A., Laurent, P. A. & Yantis, S. Value-driven attentional capture. *Proc. Natl Acad. Sci. USA* **108**, 10367–10371 (2011).
37. David, O. A. & Magurean, S. Positive attention bias trained during the rethink therapeutic online game and related improvements in children and adolescents' mental health. *Children* **9**, 1600 (2022).
38. van Rooij, S. J. H. et al. The role of the hippocampus in predicting future posttraumatic stress disorder symptoms in recently traumatized civilians. *Biol. Psychiatry* **84**, 106–115 (2018).
39. Kim, Y. J. et al. Association between posttraumatic stress disorder severity and amygdala habituation to fearful stimuli. *Depress. Anxiety* **36**, 647–658 (2019).
40. Wicking, M. et al. Deficient fear extinction memory in posttraumatic stress disorder. *Neurobiol. Learn. Mem.* **136**, 116–126 (2016).
41. Chaposhloo, M. et al. Altered resting-state functional connectivity in the anterior and posterior hippocampus in post-traumatic stress disorder: the central role of the anterior hippocampus. *NeuroImage Clin.* **38**, 103417 (2023).
42. Stevens, J. S. et al. Episodic memory after trauma exposure: medial temporal lobe function is positively related to re-experiencing and inversely related to negative affect symptoms. *NeuroImage Clin.* **17**, 650–658 (2018).
43. Tanriverdi, B. et al. Hippocampal threat reactivity interacts with physiological arousal to predict PTSD symptoms. *J. Neurosci.* **42**, 6593–6604 (2022).
44. Garavan, H., Ross, T. J. & Stein, E. A. Right hemispheric dominance of inhibitory control: an event-related functional MRI study. *Proc. Natl Acad. Sci. USA* **96**, 8301–8306 (1999).

45. van Rooij, S. J. H., Geuze, E., Kennis, M., Rademaker, A. R. & Vink, M. Neural correlates of inhibition and contextual cue processing related to treatment response in PTSD. *Neuropsychopharmacology* **40**, 667–675 (2015).
46. Luijten, M., Meerkerk, G.-J., Franken, I. H. A., van de Wetering, B. J. M. & Schoenmakers, T. M. An fMRI study of cognitive control in problem gamers. *Psychiatry Res.* **231**, 262–268 (2015).
47. Solanto, M. V., Schulz, K. P., Fan, J., Tang, C. Y. & Newcorn, J. H. Event-related FMRI of inhibitory control in the predominantly inattentive and combined subtypes of ADHD. *J. Neuroimaging* **19**, 205–212 (2009).
48. Powers, A. et al. Right inferior frontal gyrus and ventromedial prefrontal activation during response inhibition is implicated in the development of PTSD symptoms. *Eur. J. Psychotraumatology* **13**, 2059993 (2022).
49. van Rooij, S. J. H. et al. Impaired right inferior frontal gyrus response to contextual cues in male veterans with PTSD during response inhibition. *J. Psychiatry Neurosci.* **39**, 330–338 (2014).
50. Grieder, M. et al. Right inferior frontal activation during alcohol-specific inhibition increases with craving and predicts drinking outcome in alcohol use disorder. *Front. Psychiatry* **13**, 909992 (2022).
51. Kleerekooper, I. et al. The effect of aging on fronto-striatal reactive and proactive inhibitory control. *NeuroImage* **132**, 51–58 (2016).
52. Admon, R. et al. Imbalanced neural responsivity to risk and reward indicates stress vulnerability in humans. *Cereb. Cortex* **23**, 28–35 (2013).
53. Vythilingam, M. et al. Reward circuitry in resilience to severe trauma: an fMRI investigation of resilient special forces soldiers. *Psychiatry Res.* **172**, 75–77 (2009).
54. Ben-Zion, Z. et al. Neural responsivity to reward versus punishment shortly after trauma predicts long-term development of posttraumatic stress symptoms. *Biol. Psychiatry Cogn. Neurosci. Neuroimaging* **7**, 150–161 (2022).
55. Elliott, M. L. et al. What is the test–retest reliability of common task-functional mri measures? new empirical evidence and a meta-analysis. *Psychol. Sci.* **31**, 792–806 (2020).
56. Ben-Zion, Z. et al. Evaluating the evidence for brain-based biotypes of psychiatric vulnerability in the acute aftermath of trauma. *Am. J. Psychiatry* **180**, 146–154 (2023).
57. Bernstein, D. P., Ahluvalia, T., Pogge, D. & Handelsman, L. Validity of the Childhood Trauma Questionnaire in an adolescent psychiatric population. *J. Am. Acad. Child Adolesc. Psychiatry* **36**, 340–348 (1997).
58. Connor, K. M. & Davidson, J. R. T. Development of a new resilience scale: the Connor–Davidson Resilience Scale (CD-RISC). *Depress. Anxiety* **18**, 76–82 (2003).
59. Association for the Advancement of Automotive Medicine. *Abbreviated Injury Scale (c) 2005 Update 2008* (eds Gennarelli, T. & Woodzin, E.) (AAAM, 2016).
60. Bortsov, A. V. et al. Pain distribution and predictors of widespread pain in the immediate aftermath of motor vehicle collision. *Eur. J. Pain* **17**, 1243–1251 (2013).
61. Pilkonis, P. A. et al. Item banks for measuring emotional distress from the Patient-Reported Outcomes Measurement Information System (PROMIS): depression, anxiety, and anger. *Assessment* **18**, 263–283 (2011).
62. PROMIS. *HealthMeasures* https://www.healthmeasures.net/score-and-interpret/interpret-scores/promis
63. Blevins, C. A., Weathers, F. W., Davis, M. T., Witte, T. K. & Domino, J. L. The posttraumatic stress disorder checklist for dsm-5 (PCL-5): development and initial psychometric evaluation. *J. Trauma. Stress* **28**, 489–498 (2015).
64. Hamilton, C. M. et al. The PhenX Toolkit: get the most from your measures. *Am. J. Epidemiol.* **174**, 253–260 (2011).
65. Cyders, M. A., Littlefield, A. K., Coffey, S. & Karyadi, K. A. Examination of a short English version of the UPPS-P Impulsive Behavior Scale. *Addict. Behav.* **39**, 1372–1376 (2014).
66. Stevens, J. S. et al. Disrupted amygdala–prefrontal functional connectivity in civilian women with posttraumatic stress disorder. *J. Psychiatr. Res.* **47**, 1469–1478 (2013).
67. Delgado, M. R., Nystrom, L. E., Fissell, C., Noll, D. C. & Fiez, J. A. Tracking the hemodynamic responses to reward and punishment in the striatum. *J. Neurophysiol.* **84**, 3072–3077 (2000).
68. Pruim, R. H. R., Mennes, M., Buitelaar, J. K. & Beckmann, C. F. Evaluation of ICA-AROMA and alternative strategies for motion artifact removal in resting state fMRI. *NeuroImage* **112**, 278–287 (2015).
69. Hammers, A. et al. Three-dimensional maximum probability atlas of the human brain, with particular reference to the temporal lobe. *Hum. Brain Mapp.* **19**, 224–247 (2003).
70. Jovanovic, T. et al. Reduced neural activation during an inhibition task is associated with impaired fear inhibition in a traumatized civilian sample. *Cortex J. Devoted Study Nerv. Syst. Behav.* **49**, 1884–1891 (2013).
71. Tyszka, J. M. & Pauli, W. M. In vivo delineation of subdivisions of the human amygdaloid complex in a high-resolution group template. *Hum. Brain Mapp.* **37**, 3979–3998 (2016).
72. Hammers atlas database. *Brain Development* https://brain-development.org/brain-atlases/.
73. An in vivo high resolution atlas of the subcortical human brain. *OSF* https://osf.io/r2hvk/wiki/home/.
74. Maldjian, J. A., Laurienti, P. J., Kraft, R. A. & Burdette, J. H. An automated method for neuroanatomic and cytoarchitectonic atlas-based interrogation of fMRI data sets. *NeuroImage* **19**, 1233–1239 (2003).
75. Gorgolewski, K. J. et al. NeuroVault.org: a web-based repository for collecting and sharing unthresholded statistical maps of the brain. *Front. Neuroinform.* **9**, 8 (2015).
76. van Rooij, S. J. rfactor. *GitHub* https://github.com/sjhvanrooij/rfactor (2023).

Acknowledgements

The investigators thank the trauma survivors participating in the AURORA study. Their time and effort during a challenging period of their lives make our efforts to improve recovery for future trauma survivors possible. The AURORA project was supported by the National Institute of Mental Health (NIMH) under U01MH110925, the US Army MRMC, One Mind, and the Mayday Fund. The authors that were supported financially by funding for the AURORA project are as follows: R.C.K., K.J.R., K.C.K., S.A.M., S.L.H., F.L.B., X.A., J.S.S., T.C.N., G.D.C., T.J., S.D.L., L.T.G., K.A.B., S.L.R., J.P.H., A.B.S., C.L., P.I.M., P.L.H., S.S., C.W.J., B.E.P., R.A.S., V.P.M., J.L.P., M.J.S., E.H., C.P., D.A.P., R.C.M., R.M.D., N.K.R., B.J.O., L.D.S., S.E.B., J.J., D.A.P., J.F.S. and S.E.H. This paper was also supported by the NIMH under K01MH121653 (S.J.H.R.). The content is solely responsibility of the authors and does not necessarily represent the official views of any of the funders. The funders had no role in study design, data collection and analysis, decision to publish or preparation of the manuscript. Verily Life Sciences and Mindstrong Health provided some of the hardware and software used to perform study assessments. The Many Brains Project provided software for neurocognitive assessments. This paper reflects the views of the authors and may not reflect the opinions or views of the NIH or of the submitters submitting original data to the NIMH Data Archive (NDA).

Author contributions

S.A.M., R.C.K., K.J.R., K.C.K., S.J.H.v.R., J.S.S., J.L.S., C.A.H., T.D.E., N.H., V.M., L.L., T.J., S.L.H. and S.B. contributed to the conceptualization, including formulation or evolution of overarching research goals

and aims, of the study. F.L.B., X.A., T.C.N., G.D.C., S.D.L., L.T.G., K.A.B., S.L.R., J.J., D.A.P., J.F.S., S.E.H., S.A.M., R.C.K., K.J.R., K.C.K., S.J.H.v.R., J.S.S, J.L.S., C.A.H., T.D.E., N.H., V.M., L.L., T.J., S.L.H. and S.B. contributed to the methodology of the study, including development or design of methodology and creation of models. S.J.H.v.R., J.S.S, J.L.S., C.A.H., T.D.E., N.H., V.M., L.L., T.J., S.L.H., S.B. and K.J.R. contributed to the neuroimagingdata collection, formal analyses and validation of the study. S.L.H., F.L.B., X.A., J.S.S., T.C.N., G.D.C., T.J., S.D.L., L.T.G., K.A.B., S.L.R., J.P.H., A.B.S., C.L., P.I.M.Jr, P.L.H., S.S., C.W.J., B.E.P., R.A.S., J.L.P., M.J.S., E.H., C.P., D.A.P., R.C.M., R.M.D., N.K.R., B.J.O., L.D.S., S.A.M., R.C.K., K.J.R. and K.C.K. conducted the research and investigation process, specifically, performing the experiments or data and evidence collection. S.L.H., F.L.B., X.A., J.S.S., T.C.N., G.D.C., T.J., S.D.L., L.T.G., K.A.B., S.L.R., J.P.H., A.B.S., C.L., P.I.M.Jr, P.L.H., S.S., C.W.J., B.E.P., R.A.S., J.L.P., M.J.S., E.H., C.P., D.A.P., R.C.M., R.M.D., N.K.R., B.J.O., L.D.S., S.A.M., R.C.K., K.J.R. and K.C.K. provided the resources for the study, including provision of study materials, patients, laboratory samples, instrumentation, computing resources or other analysis tools. S.L.H., F.L.B., X.A., J.S.S., T.C.N., G.D.C., T.J., S.D.L., L.T.G., K.A.B., S.L.R., S.A.M., R.C.K., K.J.R. and K.C.K. were responsible for data curation, including management activities to annotate, scrub data and maintain research data for initial use and later reuse. S.J.H.v.R., J.S.S., J.L.S., C.A.H., N.H., T.J. and K.J.R. were responsible for writing the original draft, including prepration, creation and presentation of the published work, and writing initial draft. All authors contributed to the paper by reviewing and editing the original draft. S.J.H.v.R., J.S.S., J.L.S. and C.A.H. were responsible for data visualization, including preparing, creating and presenting the published work, specifically, visualization and data presentation. S.A.M., R.C.K., K.J.R., K.C.K., S.J.H.v.R. and J.S.S. were responsible for supervision, including oversight and leadership for the research activity planning and execution, including mentorship external to the core team. S.L.H., F.L.B., J.S.S., T.J., J.P.H., A.B.S., C.L. P.I.M.Jr, P.L.H., S.S., C.W.J., B.E.P., R.A.S., J.L.P., M.J.S., E.H., C.P., D.A.P., R.C.M., R.M.D., N.K.R., N.J.O., L.D.S. and S.B. were responsible for project administration, including management and coordination, responsibility for the research activity planning and execution. S.A.M., R.C.K., K.J.R. and K.C.K. were responsible for acquisition of the financial support for the project leading to this publication. S.J.H.v.R. was responsible for funding supporting her effort on this publication.

Competing interests

T.C.N. has received research support from NIH, VA and Rainwater Charitable Foundation and consulting income from Jazz Pharmaceuticals. In the past 3 years, G.D.C. has received research funding from the NSF, NIH and LifeBell AI and unrestricted donations from AliveCor Inc., Amazon Research, the Center for Discovery, the Gates Foundation, Google, the Gordon and Betty Moore Foundation, MathWorks, Microsoft Research, Nextsense Inc, One Mind Foundation, the Rett Research Foundation and Samsun Research. G.D.C. has financial interest in AliveCor Inc. and Nextsense Inc. He is also the CTO of MindChild Medical and CSO of LifeBell AI and has ownership in both companies. These relationships are unconnected to the current work. L.T.G. receives funding from the National Institute of Mental Health (R01 MH121617) and am on the board of the Many Brains Project. Her family also has equity in Intelerad Medical Systems, Inc. S.L.R. reports grants from NIH during the conduct of the study; personal fees from the Society of Biological Psychiatry paid roles as secretary, other from Oxford University Press royalties, other from American Psychiatric Publishing Inc. royalties, other from the Veterans Administration per diem for oversight committee and other from Community Psychiatry/ Mindpath Health paid board service, including equity outside the submitted work; other from National Association of Behavioral Healthcare for paid Board service; other from Springer Publishing royalties; and Leadership roles on Board or Council for SOBP, the Anxiety and Depression Association of America and the National Network of Depression Centers. S.S. has received funding from the Florida Medical Malpractice Joint Underwriter's Association Dr. Alvin E. Smith Safety of Healthcare Services Grant, Allergan Foundation, the NIH/NIA-funded Jacksonville Aging Studies Center (JAX-ASCENT; R33AG05654), the Substance Abuse and Mental health Services Administration (1H79TI083101-01) and the Florida Blue Foundation. C.W.J. has no competing interest related to this work, though he has been an investigator on studies funded by AstraZeneca, Vapotherm, Abbott and Ophirex. J.J. receives consulting payments from Janssen Pharmaceuticals. Over the past 3 years, D.A.P. has received consulting fees from Albright Stonebridge Group, Boehringer Ingelheim, Compass Pathways, Concert Pharmaceuticals, Engrail Therapeutics, Neumora Therapeutics (former BlackThorn Therapeutics), Neurocrine Biosciences, Neuroscience Software, Otsuka Pharmaceuticals and Takeda Pharmaceuticals; honoraria from the Psychonomic Society (for editorial work) and Alkermes, and research funding from NIMH, Dana Foundation, Brain and Behavior Research Foundation and Millennium Pharmaceuticals. In addition, he has received stock option from Neumora Therapeutics (former BlackThorn Therapeutics), Compass Pathways, Engrail Therapeutics, and Neuroscience Software. S.E.H. has no competing interest related to this work, though in the past 3 years he has received research funding from Aptinyx and Arbor Medical Innovations and consulting payments from Aptinyx, heron Therapeutics and Eli Lilly. In the past 3 years, R.C.K. was a consultant for Cambridge Health Alliance, Canandaigua VA Medical Center, Holmusk, Partners Healthcare, Inc., RallyPoint Networks, Inc. and Sage Therapeutics. He has stock options in Cerebral Inc., Mirah, PYM and Roga Sciences. K.C.K's research has been supported by the Robert Wood Johnson Foundation, the Kaiser Family Foundation, the Harvard Center on the Developing Child, Stanley Center for Psychiatric Research at the Broad Institute of MIT and Harvard, the NIH, One Mind, The Anonymous Foundation and Cohen Veterans Bioscience. She has been a paid consultant for Baker Hostetler, Discovery Vitality and the Department of Justice. She has been a paid external reviewer for the Chan Zuckerberg Foundation, the University of Cape Town and Capita Ireland. She has had paid speaking engagements in the past 3 years with the American Psychological Association, European Central Bank. Sigmund Freud University—Milan, Cambridge Health Alliance and Coverys. She receives royalties from Guilford Press and Oxford University Press. S.A.M. served as a consultant for Walter Reed Army Institute for Research and for Arbor Medical Innovations. K.J.R. has performed scientific consultation for Bioxcel, Bionomics, Acer and Jazz Pharm; serves on Scientific Advisory Boards for Sage, Boehringer Ingelheim, Senseye and the Brain Research Foundation; and has received sponsored research support from Alto Neuroscience. The other authors declare no competing interests.

Additional information

Supplementary information The online version contains supplementary material available at https://doi.org/10.1038/s44220-024-00242-0.

Correspondence and requests for materials should be addressed to Sanne J. H. van Rooij.

Peer review information *Nature Mental Health* thanks Saurabh Shaw, Liliane Vilete and the other, anonymous, reviewers for their contribution to the peer review of this work.

[1]Department of Psychiatry and Behavioral Sciences, Emory University School of Medicine, Atlanta, GA, USA. [2]Division of Depression and Anxiety, McLean Hospital, Belmont, MA, USA. [3]Department of Psychiatry, Harvard Medical School, Boston, MA, USA. [4]Department of Psychology, Temple University, Philadelphia, PA, USA. [5]Department of Psychiatry and Behavioral Neurosciences, Wayne State University, Detroit, MI, USA. [6]Department of Emergency Medicine, Washington University School of Medicine, St. Louis, MO, USA. [7]Department of Psychological Sciences, University of Missouri—St. Louis, St. Louis, MO, USA. [8]Department of Epidemiology, Brown University, Providence, RI, USA. [9]Department of Emergency Medicine, Brown University, Providence, RI, USA. [10]Institute for Trauma Recovery, Department of Anesthesiology, University of North Carolina at Chapel Hill, Chapel Hill, NC, USA. [11]Departments of Psychiatry and Neurology, University of California San Francisco, San Francisco, CA, USA. [12]Department of Biomedical Informatics, Emory University School of Medicine, Atlanta, GA, USA. [13]Institute for Technology in Psychiatry, McLean Hospital, Belmont, MA, USA. [14]The Many Brains Project, Belmont, MA, USA. [15]Department of Psychology and Neuroscience and Department of Sociology, University of North Carolina at Chapel Hill, Chapel Hill, NC, USA. [16]Department of Emergency Medicine, University of Massachusetts Chan Medical School, Worcester, MA, USA. [17]Department of Emergency Medicine, Vanderbilt University Medical Center, Nashville, TN, USA. [18]Department of Emergency Medicine, Henry Ford Health System, Detroit, MI, USA. [19]Department of Emergency Medicine, Indiana University School of Medicine, Indianapolis, IN, USA. [20]Department of Emergency Medicine, University of Florida College of Medicine—Jacksonville, Jacksonville, FL, USA. [21]Department of Emergency Medicine, Cooper Medical School of Rowan University, Camden, NJ, USA. [22]Department of Emergency Medicine, Ohio State University College of Medicine, Columbus, OH, USA. [23]Ohio State University College of Nursing, Columbus, OH, USA. [24]Department of Emergency Medicine, Oakland University William Beaumont School of Medicine, Rochester, MI, USA. [25]Department of Surgery, Department of Neurosurgery, University of Pennsylvania, Philadelphia, PA, USA. [26]Perelman School of Medicine, University of Pennsylvania, Philadelphia, PA, USA. [27]Department of Surgery, Division of Traumatology, Surgical Critical Care and Emergency Surgery, University of Pennsylvania, Philadelphia, PA, USA. [28]Department of Emergency Medicine, Einstein Medical Center, Philadelphia, PA, USA. [29]Department of Emergency Medicine, Wayne State University, Ascension St. John Hospital, Detroit, MI, USA. [30]Department of Emergency Medicine, Massachusetts General Hospital, Boston, MA, USA. [31]Department of Emergency Medicine, Brigham and Women's Hospital, Boston, MA, USA. [32]Department of Emergency Medicine, Trinity Health—Ann Arbor, Ypsilanti, MI, USA. [33]Department of Emergency Medicine, University of Massachusetts Medical School—Baystate, Springfield, MA, USA. [34]Department of Emergency Medicine, Wayne State University, Detroit Receiving Hospital, Detroit, MI, USA. [35]Department of Emergency Medicine, Harvard Medical School, Boston, MA, USA. [36]Department of Psychology, Yale University, New Haven, CT, USA. [37]Division of Biosciences, Ohio State University College of Dentistry, Columbus, OH, USA. [38]Institute for Behavioral Medicine Research, Ohio State University Wexner Medical Center, Columbus, OH, USA. [39]Department of Anesthesiology, University of Michigan Medical School, Ann Arbor, MI, USA. [40]Department of Internal Medicine—Rheumatology, University of Michigan Medical School, Ann Arbor, MI, USA. [41]Department of Health Care Policy, Harvard Medical School, Boston, MA, USA. [42]Department of Epidemiology, Harvard T.H. Chan School of Public Health, Harvard University, Boston, MA, USA. [43]Department of Emergency Medicine, University of North Carolina at Chapel Hill, Chapel Hill, NC, USA. ✉e-mail: sanne.van.rooij@emory.edu

nature portfolio

Corresponding author(s): Sanne J.H. van Rooij

Last updated by author(s): 2024.03.04

Reporting Summary

Nature Portfolio wishes to improve the reproducibility of the work that we publish. This form provides structure for consistency and transparency in reporting. For further information on Nature Portfolio policies, see our Editorial Policies and the Editorial Policy Checklist.

Statistics

For all statistical analyses, confirm that the following items are present in the figure legend, table legend, main text, or Methods section.

n/a	Confirmed
☐	☒ The exact sample size (*n*) for each experimental group/condition, given as a discrete number and unit of measurement
☐	☒ A statement on whether measurements were taken from distinct samples or whether the same sample was measured repeatedly
☐	☒ The statistical test(s) used AND whether they are one- or two-sided *Only common tests should be described solely by name; describe more complex techniques in the Methods section.*
☐	☒ A description of all covariates tested
☐	☒ A description of any assumptions or corrections, such as tests of normality and adjustment for multiple comparisons
☐	☒ A full description of the statistical parameters including central tendency (e.g. means) or other basic estimates (e.g. regression coefficient) AND variation (e.g. standard deviation) or associated estimates of uncertainty (e.g. confidence intervals)
☐	☒ For null hypothesis testing, the test statistic (e.g. *F*, *t*, *r*) with confidence intervals, effect sizes, degrees of freedom and *P* value noted *Give P values as exact values whenever suitable.*
☒	☐ For Bayesian analysis, information on the choice of priors and Markov chain Monte Carlo settings
☒	☐ For hierarchical and complex designs, identification of the appropriate level for tests and full reporting of outcomes
☐	☒ Estimates of effect sizes (e.g. Cohen's *d*, Pearson's *r*), indicating how they were calculated

Our web collection on statistics for biologists contains articles on many of the points above.

Software and code

Policy information about availability of computer code

Data collection	The Mindstrong DiscoveryTM Android/iOS smartphone app (iOS version 2.2; Android version 1.5.1) was used to collect clinical data. It was downloaded from the App Store (iOS users) or from Google Play (Android users) onto the participant's smartphone. Functional magnetic resonance imaging (fMRI) data was preprocessed with fMRIPrep, version 1.2.2. First and second level fMRI analyses were performed using Statistical Parametric Mapping (SPM12). Statistical Package for the Social Sciences (SPSS) version 28.0 was used for the statistical analyses. Data and/or research tools used in the preparation of this manuscript were obtained from the National Institute of Mental Health (NIMH) Data Archive (NDA). NDA is a collaborative informatics system created by the National Institutes of Health to provide a national resource to support and accelerate research in mental health. Dataset identifier(s): NIMH Data Archive Digital Object Identifier (DOI) 10.15154/zwyn-rb26. We agree to make materials, data, and associated protocols promptly available without undue qualifications
Data analysis	We agree to make code promptly available without undue qualifications. More information is available at: https://github.com/sjhvanrooij/rfactor.

For manuscripts utilizing custom algorithms or software that are central to the research but not yet described in published literature, software must be made available to editors and reviewers. We strongly encourage code deposition in a community repository (e.g. GitHub). See the Nature Portfolio guidelines for submitting code & software for further information.

Data

Policy information about availability of data

All manuscripts must include a data availability statement. This statement should provide the following information, where applicable:

- Accession codes, unique identifiers, or web links for publicly available datasets
- A description of any restrictions on data availability
- For clinical datasets or third party data, please ensure that the statement adheres to our policy

Data and/or research tools used in the preparation of this manuscript were obtained from the National Institute of Mental Health (NIMH) Data Archive (NDA). NDA is a collaborative informatics system created by the National Institutes of Health to provide a national resource to support and accelerate research in mental health. Dataset identifier(s): NIMH Data Archive Digital Object Identifier (DOI) 10.15154/zwyn-rb26. We agree to make materials, data, and associated protocols promptly available without undue qualifications.

Research involving human participants, their data, or biological material

Policy information about studies with human participants or human data. See also policy information about sex, gender (identity/presentation), and sexual orientation and race, ethnicity and racism.

Reporting on sex and gender	Biological sex assigned at birth is reported in the manuscript by means of self-report. This information is included in the manuscript. The study sample consists of 63% women. Analyses were conducted to investigate the effect of biological sex. The rationale for analyzing data across sexes is included in the manuscript.
Reporting on race, ethnicity, or other socially relevant groupings	Race/ethnicity is reported in the manuscript and the self-report method by means of self-report. This information is included in the manuscript. The data reflects a diverse sample and information on the distribution of race/ethnicity is presented. Additionally, self-report measures of marital status, education level and employment were included. Sensitivity analyses were conducted including the variables biological sex and age as covariates in the neuroimaging analyses.
Population characteristics	See above (Behavioral & Social Sciences study design)
Recruitment	Participants with trauma exposure, defined for this study as a traumatic event requiring evaluation at an Emergency Department (ED), were approached within 72 hours of their event. Research assistants (RAs) stationed in participating EDs evaluate patients for enrollment and, if eligible, inform patients about the general nature of the study, expectations for participation, and the voluntary nature of participation, and discuss risks and benefits before seeking written informed consent. There is a risk of self-selection for participants who were not interested to be enrolled in the study for any reason.
Ethics oversight	The Institutional Review Board (IRB) of the University of North Carolina (UNC) approved the study protocol (IRB #1707-03) as a multi-site human subject study on May 12, 2017 and other sites created either reliance agreements or parallel IRBs. All participants provided written informed consent. An independent medical study monitor reviewed and approved the standard operating procedures associated with evaluating and managing individuals reporting clinical worsening or as identified by study personallel. The monitor also reviewed written reports detailing participant contacts by experienced clinicians.

Note that full information on the approval of the study protocol must also be provided in the manuscript.

Field-specific reporting

Please select the one below that is the best fit for your research. If you are not sure, read the appropriate sections before making your selection.

☐ Life sciences ☒ Behavioural & social sciences ☐ Ecological, evolutionary & environmental sciences

For a reference copy of the document with all sections, see nature.com/documents/nr-reporting-summary-flat.pdf

Behavioural & social sciences study design

All studies must disclose on these points even when the disclosure is negative.

Study description	Quantitative longitudinal observational study. Details of the study design are described in McLean et al (2020).
Research sample	Patients aged 18–75 years who present to the Emergency Department (ED) within 72 hours of trauma exposure. Mean age is 37.4 (SD13.6), 64% female, 50% non-hispanic Black, 36% non-hispanic white and 10% Hispanic white. Most participants (73.5%) experienced a motor vehicle accident. This study sample of participants in the early aftermath of trauma was chosen to investigate critical changes in neurobiology and brain function that increase the risk for trauma-related psychopathology in the weeks or months after trauma. The goal was to enroll a sample representative of the US population.
Sampling strategy	The study is a quantitative longitudinal observational study. The experiments were not randomized and the investigators were not blinded to outcome assessments. Patients who presented to the ED within 72 hours of trauma exposure at participating ED sites were screened for study eligibility. The goal was to enroll 5,000 participants in the study, with adaptive sampling of specific trauma subsamples and adjustment of study design over the course of the study as necessary to achieve study goals. The study was not powered to address a specific hypothesis, instead, given the fixed budget and multiple study aims, the study was designed to have

	the largest possible sample size while collecting all the types of data needed to address the aims of the parent project, which included identifying and characterizing trajectories of the most common trauma-induced symptoms across mental and physical health domains, and to conduct machine learning to identify individuals at high risk of adverse outcomes following trauma. The study concluded in December 2020 with a final sample of n=2,943 with follow-up data. Data for the current manuscript included participants with complete 6-month follow-up data (n=1835). Subsamples of study participants who lived within driving distance of an AURORA neuroimaging/deep phenotyping site were asked to return for in-person evaluations two weeks after the ED visit (n=445 total) A total of n=260 are included in the neuroimaging analyses (after excluding for anatomical concerns, lack of behavioral responses or available data, excessive motion, technical issues, or incomplete resilience factor data). Power analyses for neuroimaging data are included in the Supplemental Materials S1.
Data collection	ED assessments were conducted by trained research assistants. There were no restrictions to the presence of other individuals including hospital personnel or family members or friends. There were no experimental conditions or specific study hypotheses, but the research assistants were aware of the general study goals. Participants completed interview and self-administered surveys in the ED. Participants also had an Android/iOS smartphone app downloaded onto their smartphone. Follow-up surveys were completed 2-weeks, 8-weeks, 3-months, 6-months, and 12-months after initial evaluation via web-based or phone assessments via self-report surveys. A subset of participants was invited for the MRI scan 2 weeks after enrollment in the ED.
Timing	The first time point for data collection was within 72 hours of trauma exposure in the ED. Follow-up assessments were completed 2-weeks, 8-weeks, 3-months, 6-months, and 12-months after initial evaluation. For this manuscript, data collected in the ED, at 2 weeks and 6 months following trauma exposure were used. Study data was collected between 09/2017 and 12/2020.
Data exclusions	A total of n=2,943 participants were included in the AURORA study. The current investigation included n=2,772 AURORA participants with clinical item-level data at 2-weeks or 6-months recruited from 09/2017 to 12/2020. Missing data values were excluded listwise, resulting in n=1,835 (1,175 women) participants with complete 6-month item level clinical data usable for analyses. fMRI data were collected for n=445; the fMRI scan included a response inhibition paradigm (n=428), a fearful faces "social threat" task (n=431), and a monetary reward processing task (n=427). Functional data were excluded from analyses for anatomical concerns (n=7), lack of expected behavioral responses or available data (inhibition, n=45; threat, n=14; reward, n=26), excessive motion (any run with >15% of volumes exceeding 1mm FD; inhibition, n=33; threat, n=25; reward, n=45), technical issues during the scan (inhibition, n=14; threat, n=15; reward, n=24). Final data were available for n=385 for at least one of the tasks (n=329 for inhibition, n=370 for threat processing, and n=325 for reward processing). Of these, associations with resilience factor scores were investigated for n=260 individuals who had scores available (Table 1; n=215 for inhibition, n=249 for threat processing, and n=214 for reward processing). Dynamic resilience factor scores (both complete 2-week and 6-month clinical data) were investigated for respectively n=189, n=221, and n=189.
Non-participation	Total approached in ED n=22,814 (screening error n=12; system failure, n=860) Final approach n=21,942 (ineligible medical record review, n=5,566) Potentially eligible n=16,376 (refused before completion of screening, n=9,222) Completed screening, n=7,154 (ineligible based on patient screening, n=2,596) Eligible, n=4558 (refused after screening, n=729) Enrolled, n=3,829 (medical extraction incomplete or unavailable, n=36) Full enrollment, n=3,793 (enrolled less than 67 days, neither did complete week 8 survey, n=847) N=2,946 (exclusionary total drop due to pregnancy or incarceration, n=3) Final n=2,943
Randomization	The study was observational and participants were not allocated to groups.

Reporting for specific materials, systems and methods

We require information from authors about some types of materials, experimental systems and methods used in many studies. Here, indicate whether each material, system or method listed is relevant to your study. If you are not sure if a list item applies to your research, read the appropriate section before selecting a response.

Materials & experimental systems

n/a	Involved in the study
☒	☐ Antibodies
☒	☐ Eukaryotic cell lines
☒	☐ Palaeontology and archaeology
☒	☐ Animals and other organisms
☒	☐ Clinical data
☒	☐ Dual use research of concern
☒	☐ Plants

Methods

n/a	Involved in the study
☒	☐ ChIP-seq
☒	☐ Flow cytometry
☐	☒ MRI-based neuroimaging

Magnetic resonance imaging

Experimental design

Design type	Three functional MRI tasks, one block design, two event-related designs

Design specifications	Inhibition was measured using the Go/NoGo task. Participants were shown either an X or an O for 1,000ms and were instructed to press 1 for X and 2 for O (Go trials), but not press a button when a red rectangle appeared behind the X or the O (NoGo trial). The task consists of four runs with 26 Go trials, 13 NoGo trials, and 14 blank trials consisting of a black background only. Trials were presented in random order. Trials were followed by a jittered intertrial interval of 1,250-2,500ms and a 500ms fixation cross. The contrast NoGo>Go was used to measure response inhibition. Threat processing was assessed with the fearful faces task. Participants viewed blocks of static fearful and neutral faces from the Ekman and Friesen faces library. A total of 15 blocks with fearful faces and 15 blocks with neutral faces were presented in pseudorandom order, and block order was counterbalanced across participants. Each 6,000ms block consisted of eight different face simuli, each presented for 500ms with a 500ms interstimulus interval. After every 10 blocks a 10,000ms rest period occurred in which participants were instructed to relax. The fearful>neutral faces contrast was used to measure threat processing. For reward processing, a short version of Delgado's monetary reward task was used. Participants viewed a card with a question mark and were asked to indicate by a button press whether they guess the card's value would be higher or lower than 5 before the real value was revealed. A total of 40 trials were presented, each including a 2,000ms guessing period in which a button press was recorded, then the card's value and monetary outcome was presented after a 2,000-4,000ms delay. Participants were told they would win $1 for each correct guess and lose $0.50 for each incorrect guess and were told they would receive this money. Unknown to the participants, the outcome was predetermined to create 10 wins and 10 losses resulting in $10. The contrast gain>loss was used to measure reward processing.
Behavioral performance measures	The fearful faces task is a passive viewing task. Correct button presses were recorded for the reward and inhibition tasks. For the reward task, trials with no response were excluded. For the inhibition task, only correct Go and NoGo trials were included. Individuals with lack of expected behavioral responses or available data (inhibition, n=45; threat, n=14; reward, n=26) were excluded.

Acquisition

Imaging type(s)	Functional
Field strength	3T
Sequence & imaging parameters	Site 1 (Emory) Siemens TIM 3T Trio (12-channel head coil) T1-weighted: TR = 2530ms, TEs = 1.74/3.6/ 5.46/7.32ms, TI = 1260ms, flip angle = 7, FOV = 256mm, slices = 176, Voxel size = 1mm x 1mm x 1mm Functional MRI: TR = 2360ms, TE = 30ms, flip angle = 70, FOV = 212mm, slices = 44, Voxel size = 3mm x 2.72mm x 2.72mm, 0.5 mm gap Site 2 (McLean) Siemens TIM 3T Trio (12-channel head coil) T1-weighted: TR = 2530ms, TEs = 1.74/3.6/ 5.46/7.32ms, TI = 1260ms, flip angle = 7, FOV = 256mm, slices = 176, Voxel size = 1mm x 1mm x 1mm Functional MRI: TR = 2360ms, TE = 30ms, flip angle = 70, FOV = 212mm, slices = 44, Voxel size = 3mm x 3mm x 3mm, 0.5 mm gap Site 3 (Wayne) Siemens Magnetom 3T PRISMA (20-channel head coil) T1-weighted: TR = 2300ms, TE = 2.96ms, TI = 900ms, flip angle = 9, FOV = 256mm, slices = 176, Voxel size = 1.2mm x 1.0mm x 12mm Functional MRI: TR = 2360ms, TE = 29ms, flip angle = 70, FOV = 212mm, slices = 44, Voxel size = 3mm x 2.72mm x 2.72mm, 0.5 mm gap Site 4 (Temple) Siemens 3T Verio (12-channel head coil) T1-weighted: TR = 2530ms, TEs = 1.74/3.65/ 5.51/7.72ms, TI = 1260ms, flip angle = 7, FOV = 256mm, slices = 176, Voxel size = 1mm x 1mm x 1mm Functional MRI: TR = 2360ms, TE = 30ms, flip angle = 70, FOV = 212mm, slices = 42, Voxel size = 3mm x 2.72mm x 2.72mm, 0.5 mm gap Site 5 (Wash U) Siemens Magnetom 3T PRISMA (20-channel head coil) T1-weighted: TR = 2300ms, TE = 2.98ms, TI = 900ms, flip angle = 9, FOV = 256mm, slices = 176, Voxel size = 1.2mm x 1.0mm x 12mm Functional MRI: TR = 2360ms, TE = 29ms, flip angle = 90, FOV = 210mm, slices = 44, Voxel size = 3mm x 3mm x 2.5mm, 0.5 mm gap
Area of acquisition	Whole brain scan was used

Diffusion MRI ☐ Used ☒ Not used

Preprocessing

Preprocessing software	Details on MRI preprocessing are described in our prior publication (Stevens et al 2021, details in online Supplemental Materials): DICOM images were converted to NIFTI format using Brain Imaging Data Structure (BIDS) nomenclature using dcm2niix (Li et al. 2016). Visually inspection for conversion errors and data exclusion criteria was performed (e.g., signal drop-out from Falx calcification, anatomical abnormalities). Quality control was further achieved using the MRIQC pipeline (version 0.10.4 in a Docker container) (Esteban et al. 2017a) on both structural and functional images. We used fMRIPrep 1.2.2 (Esteban, Blair, et

al. (2017); Esteban, Markiewicz, et al. (2018); RRID:SCR_016216), which is based on Nipype 1.1.5 (Gorgolewski et al. (2011); Gorgolewski et al. (2017); RRID:SCR_002502). To ensure consistency in preprocessing throughout the duration of data collection, FMRIPrep was run in a Docker container retaining the version that was newest at the initiation of the study.

T1-weighted (T1w) images were corrected for intensity nonuniformity by using N4BiasFieldCorrection (Tustison et al. 2010, ANTs 2.2.0), and throughout the workflow used as T1w-reference. Next, the T1w-reference was skull-stripped using antsBrainExtraction.sh (ANTs 2.2.0), and OASIS as target template. Recon-all (FreeSurfer 6.0.1, RRID:SCR_001847, Dale, Fischl, and Sereno 1999) was used for reconstruction of brain surfaces. The previoulsy estimated brain mask was refined with a custom variation of the method to reconcile ANTs-derived and FreeSurfer-derived segmentations of the cortical gray-matter of Mindboggle (RRID:SCR_002438, Klein et al. 2017). Brain tissue segmentation of cerebrospinal fluid (CSF), white-matter (WM) and gray-matter (GM) was performed on the brain-extracted T1w using fast (FSL 5.0.9, RRID:SCR_002823, Zhang, Brady, and Smith 2001).

fMRIPrep, version 1.2.2 was used to preprocess functional images. A custom methodology of fMRIPrep was used to generate reference volume and its skull-stripped version. Next, the BOLD reference was co-registered to the T1w reference for which bbregister (FreeSurfer) was used which implements boundary-based registration (Greve and Fischl, 2009). To account for distortions remaining in the BOLD reference, co-registration was configured with nine degrees of freedom. Head-motion parameters relative to the BOLD reference (transformation matrices, and six corresponding rotation and translation parameters) were estimated before spatiotemporal filtering using mcflirt (FSL 5.0.9, Jenkinson et al. 2002). Slice-time correction was performed using 3dTshift from AFNI 20160207 (Cox, 1996, RRID:SCR_005927). Then, BOLD time-series (including slice-timing correction) were resampled onto their original, native space for which a single, composite transform was applied to correct for head-motion and susceptibility distortions. Images were smoothed with a 6-mm kernel.

Normalization

Spatial normalization to the ICBM 152 Nonlinear Asymmetrical template version 2009c (Fonov et al. 2009, RRID:SCR_008796) was performed through nonlinear registration with antsRegistration (ANTs 2.2.0, RRID:SCR_004757, Avants et al. 2008), using brain-extracted versions of both T1w volume and template.

Normalization template

2009 ICBM-152 template

Noise and artifact removal

Automatic removal of motion artifacts using independent component analysis (ICA-AROMA, Pruim et al. 2015) was performed on the preprocessed BOLD on MNI space time-series after removal of non-steady state volumes and spatial smoothing with an isotropic, Gaussian kernel of 6mm FWHM (full-width half-maximum).

Volume censoring

An overall motion threshold was implemented for any run with >15% of volumes with more than 1mm framewise displacement in order to handle cases in which motion was likely too high for effective ICA correction.

Statistical modeling & inference

Model type and settings

First-level statistical modeling was conducted in SPM12. For the Go/NoGo task, correct Go and correct NoGo trials were modeled in an event-related design (0ms event duration), and incorrect Go and NoGo trials were modeled separately. The contrast of correct NoGo > correct Go trials was used to measure response inhibition. For the fearful faces task, blocks of fearful and neutral stimuli were modeled with separate boxcar functions representing the onset and 8000 ms duration of each block, and were convolved with a canonical hemodynamic response function. The fearful > neutral face contrast was used to measure threat processing. For the card task, gain and loss trials were modeled as separate experimental conditions in an event-related design. Furthermore, each trial during which the participant did not press a button was modeled in an error condition. The Gain > Loss contrast were used to measure reward processing. In all first-level models, nuisance regressors included white matter, CSF and global signal time courses. Whole brain group level maps were created for the inhibition, threat, and reward contrasts and included dummy variables for site. Separate models were created for each factor and static and dynamic resilience.

Effect(s) tested

A factorial design with multiple regressors was used to examine correlations between the contrast estimates for inhibition, threat and reward with each of the continuous resilience factor scores as covariates in separate models.

Specify type of analysis: ☐ Whole brain ☐ ROI-based ☒ Both

Anatomical location(s)

The mean across all voxels in each ROI was extracted from first-level contrasts using rex (https://www.nitrc.org/projects/rex/). Contrast estimates were extracted for our predefined ROIs, also described in our earlier papers. Anatomical bounderies were used to define bilateral ROIs. For inhibition (NoGo>Go contrast), the hippocampus (Hammers atlas) and the ventromedial prefrontal cortex (defined based on our prior study findings; 6mm sphere around –4, 44, -4), were used. For threat processing (fearful>neutral faces contrast), the amygdala (based on the CITI168 subcortical atlas), the bilateral hippocampus (Hammers atlas), and the subgenual anterior cingulate cortex (sgACC) and dorsal ACC (dACC) respectively defined ad BA25 and BA32 (map of the BA from the WFUPickAtlas) were used. For reward processing (Gain>Loss), the nucleus accumbens and bilateral amygdala (CITI168 subcortical atlas), and orbitofrontal cortex (OFC; Harvard/Oxford atlas) were used.

Statistic type for inference

(See Eklund et al. 2016)

Whole brain analyses with a cluster-wise method was used. A primary threshold of p<0.005 combined with a Family Wise Error (FWE) cluster-level correction was applied to correct for multiple comparisons using the default in SPM12.

Correction

Two levels of corrections were applied. First, bonferroni correction using FWE cluster-level correction was applied using SPM12 default settings (see statistic type for inference). Second, bonferroni correction was applied to correct for multiple testing across the three domains (task constructs), three components (r-factor, reminder acceptance, behavioral control), and two features (static and dynamic resilience), corrected p<0.0028.

Models & analysis

n/a	Involved in the study
☒	☐ Functional and/or effective connectivity
☒	☐ Graph analysis
☒	☐ Multivariate modeling or predictive analysis